

THE $^{25}\text{Mg}(p, \gamma)^{26}\text{Al}$ REACTION; BRANCHINGS, ENERGIES AND LIFETIMES

P.M. ENDT, P. DE WIT and C. ALDERLIESTEN

Fysisch Laboratorium, Utrecht University, The Netherlands

Received 11 September 1987

Abstract: The γ -decay has been measured of 75 $^{25}\text{Mg}(p, \gamma)^{26}\text{Al}$ resonances in the $E_p = 0.31\text{--}1.84$ MeV region with Ge detectors at 90° and 55° , the latter in a Compton suppression shield. Several of these resonances had not been observed previously and of about half the decay had not been measured. The spectra have been corrected for summing effects, for the instrumental tails of lower-energy resonances, for the Breit-Wigner tails of neighbouring broad resonances, and for direct capture.

On the average about 29 primaries are observed per resonance (with a maximum of 48); 74 primaries are of the resonance \rightarrow resonance type. Altogether 109 secondary states are excited in the decay, of which 50 had been seen in previous (p, γ) work. The total number of observed decay γ -rays from non-resonance levels amounts to 548, with a maximum number of branches per level of 20.

Accurate energies have been measured for all states. The errors amount to $\Delta E_x = 0.03\text{--}0.26$ keV for the non-resonance levels and to $0.04\text{--}0.4$ keV for the resonances (with $\Delta E_x = 2$ keV for four very broad resonances).

As a byproduct lifetimes (or lifetime limits) have been measured from the observed Doppler shifts for 32 levels for which no previous measurements existed.

E

NUCLEAR STRUCTURE $^{25}\text{Mg}(p, \gamma)$, $E = 0.31\text{--}1.84$ MeV; measured $\sigma(E, E_\gamma)$. ^{26}Al deduced levels, γ -branchings, $T_{1/2}$. Enriched targets, Ge detectors.

1. Introduction

In a previous paper ¹⁾ the existence, yields and partial widths have been discussed of $^{25}\text{Mg}(p, \gamma)^{26}\text{Al}$ and $^{25}\text{Mg}(p, p')^{25}\text{Mg}$ resonances in the $E_p = 0.31\text{--}1.84$ MeV region. In the present paper the γ -ray branchings and energies are given of (p, γ) resonances and secondary states, and DSA lifetimes of the latter. The most extensive previous investigation of the $^{25}\text{Mg}(p, \gamma)$ reaction is by De Neys *et al.* ²⁾ who measured spectra at 44 resonances with altogether about 500 primaries (present work 2200), and 133 transitions between bound states (present work 548).

The data obtained in ref. ¹⁾ and in the present paper form the basis for spin, parity and isospin determinations, and (for the even-parity states) for a comparison with a shell-model calculation of energies and transition probabilities to be discussed in a succeeding paper.

Two particular aspects of the present work, the use to be made of γ -ray strength statistics, and the usefulness of the results for nucleosynthesis have already been published^{3,24}).

2. Experimental

For details on the accelerator, the proton beam and on targets, see ref.¹).

At all (p, γ) resonances listed in ref.¹) Ge spectra have been taken, mostly with detectors at $\theta = 90^\circ$ and 55° , the latter in an anti-Compton shield. Energies were obtained from the spectra at 90° , where lines are not Doppler shifted, and intensities from the spectra at 55° , where $P_2(\cos \theta)$ is equal to zero. In all these 8k-channel spectra the dispersion amounted to about 1 keV per channel.

Four different Ge detectors have been used; two n-type hyperpure Ge detectors of 90 and 95 cm³ active volume, a p-type hyperpure Ge detector of 90 cm³, and a 125 cm³ Ge(Li) detector. Particulars on the Compton suppression spectrometer (CSS) with good Compton suppression (suppression factor about 11 for ^{60}Co) and relatively large solid angle ($\Delta\Omega = 65$ msr for a target-to-collimator front face distance of 3 cm) are given in ref.⁴). For the present investigation (with E_γ up to 8 MeV) the thickness of the front plate lead shielding was increased by 2 cm. We may add that for the 125 cm³ detector the intensity ratio of double- to single-escape pair peaks amounted to about 0.015. Energy resolution, to be judged by the quality of the spectra given in sects. 3 and 4, depended on the detector and on time; some detectors have deteriorated in the course of the five years of the present experiment and had to be regenerated.

The γ -ray line width is not only determined by the instrumental resolution. The decay lines of levels with lifetimes in the $\tau_m \approx 100$ –200 fs region, corresponding to $F(\tau_m) \approx 0.4$ –0.6, are visibly Doppler broadened in the 55° spectra, with the intrinsic width of the Doppler structure comparable to the instrumental width. In addition, primaries are broadened at resonances with an appreciable natural width (if the target is not very thin). Examples of lines broadened by these two causes are given in fig. 1.

Decay lines from short-lived levels (for instance, resonance primaries) should also be broadened because of the finite detector opening angle, especially at $\theta = 90^\circ$, but this effect is hardly observable, even at the highest-energy resonances.

Bombarding times were up to 30 h per resonance, with a total proton charge of up to 3200 μAh , with a minimum of 300 μAh , and an average of about 1000 μAh per resonance. At several resonances, in particular at weak resonances which were previously unobserved, first short runs were performed to see whether the resonance was due to $^{25}\text{Mg}(p, \gamma)$, to be followed by long runs especially if the resonance proved interesting with relatively strong branches to unusual levels. Because of the differences in resonance strengths and bombarding times, the resulting spectra have widely different statistical qualities (as measured by the intensity sum of all

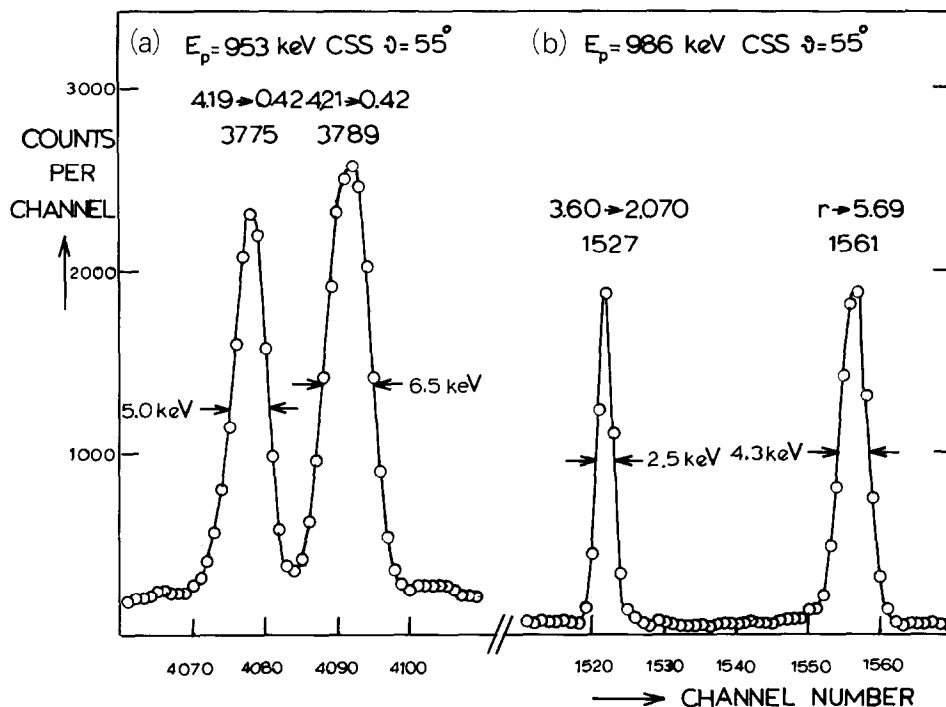


Fig. 1. Examples of broadened lines. (a) The $4.21 \rightarrow 0.42$ MeV secondary is Doppler broadened, as seen by comparison with the unbroadened $4.19 \rightarrow 0.42$ MeV transition. (b) The $r \rightarrow 5.69$ MeV primary at the $E_p = 986$ keV resonance is broadened because of the non-negligible resonance width ($\Gamma = 3.4$ keV); the $3.60 \rightarrow 2.070$ MeV transition is unbroadened.

primaries), with the best and the poorest differing by as much as a factor 10^4 . At higher proton energies some spectra are deteriorated by the presence of strong $E_\gamma = 585$ and/or 975 keV lines from $^{25}\text{Mg}(p, p')$. At the $E_p = 1568$ resonance, for example, the $E_\gamma = 585$ keV intensity exceeds the primary intensity sum by a factor 2000. The same effect would also make the extension of the (p, γ) work to $E_p > 1.84$ MeV quite difficult.

Background measurements at a few keV below the resonance in question have been performed in a few cases, but they did not prove very useful, mainly because the strongly resonant nature of part of the contaminant reactions, like e.g. $^{26}\text{Mg}(p, \gamma)$.

The most common contaminants have already been discussed in ref. ¹). In addition, we might mention the (p, p') reactions on ^{19}F ($E_\gamma = 197$ keV), on ^{23}Na ($E_\gamma = 440$ keV) and on ^{181}Ta ($E_\gamma = 136, 165$ and 301 keV), and the radioactive contaminants of the target holder ^7Be (53 d, $E_\gamma = 478$ keV), ^{48}Sc (44 h, $E_\gamma = 983, 1037$ and 1312 keV), ^{65}Zn (244 d, $E_\gamma = 1116$ keV), and ^{182}Ta (115 d, $E_\gamma = 1121, 1189, 1221$ and 1231 keV), produced through (p, α) , (p, n) and (d, p) reactions by other users of the accelerator.

Spectra were taken in runs of about 1 h and stored on magnetic tape via a PDP 11/34 computer. For details of the data acquisition, see ref. ²²). These subspectra

were later computer added, in which process possible gain and zero shifts were corrected for by fixing the positions of one relatively strong peak at low and one at high energy. At any moment during the measurements the spectra could be examined visually to check resolution and Compton suppression, or to investigate the potential presence of possibly interesting transitions.

The final spectra have been analysed by means of an automatic peak search programme determining the position, width and number of counts of all reasonably strong isolated peaks. As a second step, weak but possibly interesting peaks and peak multiplets were fitted by means of an interactive fitting programme. Peak shapes were considered as being gaussian with an additional low-energy exponential tail.

Intensity calibrations were performed with the help of standard radioactive sources⁵), and with the (p, γ) reactions on ^{23}Na and ^{27}Al [ref. 6)].

The lines used for the energy calibration are discussed in sect. 5. As a first approximation to an energy calibration curve a straight line was drawn through a calibration point at low and one at high energy. The deviations of the other calibration points from this line were then plotted on much enlarged scale. The usual shape of the smooth calibration curve hand-fitted to the calibration points is that of an asymmetric parabola, but also curves have been observed of a tilted-S shape (a bump and a valley), or even of camel shape (two bumps with a valley in between), depending on the amplifier-ADC combination used. The best curves had a deviation from the first-approximation straight line of less than 1 keV over a 5000 keV region. For the worst curves the maximum deviation was ten times larger. With statistically well determined curves based on many strong calibration lines with 30–40 eV errors, energies can be determined to about the same accuracy.

The method sketched above has the advantage that a calibration peak contaminated with another as yet unspotted transition shows up clearly. This makes the method superior to, for instance, linear interpolation between two close-lying calibration points, and also to a computer fit of some polynomial in the channel number to the calibration points.

3. Resonance branchings

As already mentioned in the introduction, the present work has produced much more detailed branchings as compared to previous work. The possibility to observe weak lines, especially at low energy, is due to the good qualities of the CSS (large opening angle, good Compton suppression). As an example we give in table 1 the decay of the $E_p = 1714$ keV resonance. It shows 45 primaries with only six branchings exceeding 1%, and with the strongest and the weakest primary differing in intensity by a factor 10^4 . The eight lowest-energy primaries are all of the resonance \rightarrow resonance type. The branching errors have been obtained by compounding the statistical error with a 3% systematic error, the latter accounting for possible deficiencies in the intensity calibration.

TABLE 1

Decay of the $E_p = 1714$ keV resonance ($E_x = 7953$ keV, $J^\pi; T = 4^+; 1$)^a

E_x [keV]	$J^\pi; T$	b [%]	E_x [keV]	$J^\pi; T$	b [%]	E_x [keV]	$J^\pi; T$	b [%]
0	$5^+; 0$	74.64	4192	$3^+; 1$	0.0996	5545	$2^+; 1$	<0.04
417	$3^+; 0$	0.813	4206	$4^+; 0$	0.0166	5569	$5^+(4, 3^+); 0$	0.0152
1759	$2^+; 0$	0.031	4349	$3^+; 0$	0.0374	5598	$3^-; 0$	<0.01
2069	$4^+; 0$	3.0510	4548	$2^+; 1$	<0.02	5676	$4^-; 0$	<0.02
2070	$2^+; 1$	0.188	4599	$3^+; 1$	0.2028	5692	$3^-; 0$	0.0072
2365	$3^+; 0$	9.63	4705	$4^+; 1$	0.052	5726	$4^+; 1$	0.0132
2545	$3^+; 0$	0.271	4773	$4^+; 0$	0.0293	6084	$5^+; 0$	0.0934
2661	$2^+; 0$	0.0075	4941	$5^+; 0$	0.351	6198	$2^+; 0$	0.0072
2913	$2^+; 0$	0.0095	4952	$3^+; 0$	<0.01	6343	$4^-; 0$	0.0196
3074	$3^+; 0$	0.0365	5132	$4^+; 1$	0.0533	6436	$4^-; 0$	0.2017
3160	$2^+; 1$	0.552	5142	$2^+; 1$	<0.01	6496	$5^+(4^+); 0$	0.2488
3403	$5^+; 0$	3.7611	5245	$4^+; 0$	0.0273	6551	$4^+(5^+); 0$	0.0135
3508	$6^+; 0$	0.0284	5396	$4^-; 0$	0.0283	6598	$(4, 5^+); 0$	0.0263
3596	$3^+; 0$	0.1005	5457	$3^-; 0$	<0.02	6724	$4^-; 0$	0.0072
3675	$4^+; 0$	0.022	5462	$0^+(1, 2); 0$	<0.01	6801	$3^+; 0$	0.0102
3681	$3^+; 0$	0.311	5488	$5^+(4^-); 0$	0.1576	7015	$5^+; 0$	0.0253
3751	$2^+; 0$	0.0124	5495	$2^+; 0$	<0.01	7109	$4^-; 0$	0.1024
3963	$3^+; 0$	1.144	5513	$4^+; 0$	3.5811	7291	$4^+(3^+); 0$	0.0623

^a Errors are underlined. Branching upper limits are given for unobserved levels below $E_x = 5.8$ MeV with possible primaries of dipole or E2 character.

The error introduced by making the assumption that the intensity measured at $\theta = 55^\circ$ is equal to the intensity averaged over the angular distribution has been neglected. Of the 45 primary angular distributions measured by De Neys *et al.*²⁾ at 19 resonances only three have an A_4 coefficient which significantly differs from zero, and even these coefficients are so small that the $A_4 = 0$ assumption would have introduced an error of at most 6%.

In fig. 2 we show parts of the $E_p = 1714$ keV CSS spectrum at $\theta = 55^\circ$ to demonstrate how some of the weak low-energy primaries still clearly stand out above the Compton background.

Whether a particular line in the spectrum is a primary, uncontaminated by other lines, is determined, if not by its energy, by the intensity balance at the final state. The intensity balance has also been used to derive the intensity of a contaminated primary from the observed final-state decay intensity, or to derive the intensity of a contaminated decay line from the primary intensity and the known branching of the level in question, in both cases with indirect feeding taken into account.

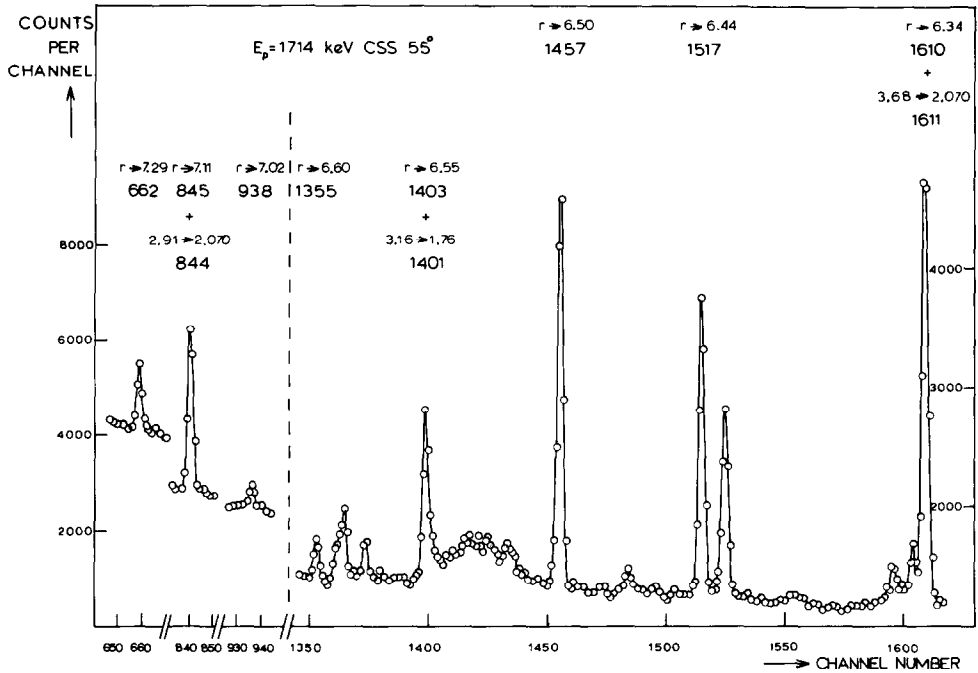


Fig. 2. Parts of the 55° CSS spectrum at the $E_p = 1714$ keV resonance showing some very weak primaries (branchings 0.025–0.25%). Unmarked peaks are produced by secondary transitions.

In table 2 an example is shown of the agreement between feeding and decay intensities (I_{in} and I_{out} , respectively; for the definition of intensity, see also table 2) obtained for the 32 final states populated at the $E_p = 390$ keV resonance ($E_x = 6680$ keV). For the reasonably strongly excited levels ($I_{in} > 60$), the average absolute value of the relative difference between I_{in} and I_{out} amounts to 2.8% which is about equal to the 3% intensity calibration error mentioned above. For the weakly excited levels ($I_{in} < 60$) we find $\langle |I_{in} - I_{out}| \rangle_{av} = 2.7$ which is close to the intensity detection limit which for this particular spectrum increases from $I \approx 1$ at $E_\gamma = 0.6$ MeV to $I \approx 2$ at $E_\gamma = 5.0$ MeV. A comparison of I_{in} and I_{out} for the states at $E_x = 0$ and 0.23 MeV is impossible, because the states decay through (unobserved) β^+ emission. Instead one can check the primary intensity sum against the sum of the I_{in} values for the two states (see table 2).

At about 30% of the investigated resonances all γ -lines of statistical significance could be placed, either as resulting from $^{25}\text{Mg} + p$ or from known contaminant reactions. The about 65 lines which have remained unplaced are all quite weak. Their intensity sum added over all resonances amounts to 0.03% of the intensity sum of all resonance primaries.

A special problem is the determination of the primary branchings for the components of the triplet at $E_x = 2.07$ MeV and the doublets at $E_x = 3.68, 3.75, 4.94$,

TABLE 2

Intensity balance for secondary states observed in the CSS spectrum ($\theta = 55^\circ$) at the
 $E_p = 390$ keV, $E_x = 6680$ keV, $2^+;0$ resonance ^a

E_{xf} [keV]	$J^\pi_f; T_f$ ^b	I_{pr}	I_{sec}	I_{in}	I_{out}	E_{xf} [keV]	$J^\pi_f; T_f$ ^b	I_{pr}	I_{sec}	I_{in}	I_{out}
0	$5^+;0$		1216	1216	c	3596	$3^+;0$		4	4	d
228	$0^+;1$	15	576	591	c	3675	$4^+;0$		11	11	11
417	$3^+;0$	115	1040	1155	1170	3681	$3^+;0$		2	2	7
1058	$1^+;0$	35	432	467	462	3724	$1^+;0$	6	2	8	4
1759	$2^+;0$	9	239	248	250	3751	$2^+;0$		20	20	23
1851	$1^+;0$	77	2	79	86	3963	$3^+;0$	3	2	5	8
2069	$4^+;0$		132	132	140	4192	$3^+;1$	520		520	513
2070	$2^+;1$	323	131	454	472	4349	$3^+;0$	12		12	9
2072	$1^+;1$		8	8	6	4548	$2^+;1$	54		54	60
2365	$3^+;0$	12	73	85	87	4599	$3^+;1$	378		378	379
2545	$3^+;0$	3	30	33	35	4952	$3^+;0$	2		2	d
2661	$2^+;0$	18	31	49	42	5132	$4^+;1$	1		1	
2740	$1^+;0$	5	2	7	3	5142	$2^+;1$	14		14	14
2913	$2^+;0$	2	20	22	21	5495	$2^+;0$	1		1	2
3074	$3^+;0$		6	6	3	5545	$2^+;1$	63		63	63
3160	$2^+;1$	99	6	105	110	6364	$3^+;1$	1		1	

^a The intensity is I defined as $I = 0.01 N/\epsilon$, where N is the number of counts in the full-energy peak, and ϵ is the detection efficiency normalized to $\epsilon = 1$ at $E_\gamma = 1$ MeV; I_{pr} and I_{sec} stand for the intensity of the primary and for the intensity sum of the secondaries feeding the level in question. The primary intensity sum $\Sigma I_{pr} = 1768$ compares well with the intensity sum of all transitions feeding the states at $E_x = 0$ and 228 keV, $\Sigma I_{in} = 1807$.

^b To be discussed in a succeeding paper.

^c Decay through (unobserved) β^+ emission.

^d Main decay lines obscured by other (stronger) lines.

5.01, 5.46, 5.49, 5.67, 5.92 and 6.08 MeV (for accurate excitation energies, see table 10). In many cases the energy of the primary (as determined at 90° or 55°) has been used, in other cases the component intensity balance gave the decision (with secondary feeding taken into account). For the 2.07 MeV triplet the intensity balance is the most important, because usually the energy calibration in the high-energy part of the spectrum is not good enough.

Another problem is formed by very weak high-energy primaries which can originate from a number of effects other than the decay of the resonance in question.

Well known is coincident summing. For instance a $r \rightarrow 0$ MeV transition can be faked by the summing of the $r \rightarrow 0.42$ and $0.42 \rightarrow 0$ MeV transitions. In the usual closest-distance geometry ($d = 3$ cm), this leads to $I(r \rightarrow 0)/I(r \rightarrow 0.42) \approx 5 \times 10^{-4}$ for the CSS.

Random summing is also observed, mainly of the strong lines from the (p, p') reactions on ^{25}Mg and ^{181}Ta . The random summing peaks have a characteristic shape with a tail on the low-energy side.

The instrumental tail of the preceding resonance(s), due to finite target thickness, and the contribution from the Breit-Wigner (BW) tails of neighbouring strong and broad resonances have already been mentioned in ref. ¹⁾. In that paper the influence of these two effects was discussed on the intensities of the $E_\gamma = 585$ and 975 keV lines resulting from the $^{25}\text{Mg}(p, p')$ reaction, but they are equally important for (p, γ) . The BW tail sum has been calculated separately for each primary, with at some energies as many as eight neighbouring resonances contributing, and with the interference between resonances with the same J^π ; T value taken into account ⁹⁾. This laborious calculation, necessitated by the fact that the weak primaries are often instrumental in the determination of resonance spins and/or parities, is made possible by the present extensive knowledge on resonance strengths, widths and J^π ; T values ¹⁾.

An effect, which as far as we know has not yet been described in the literature, is the appearance of weak γ -ray peaks corresponding to the strongest primaries of resonances often as far as several 100 keV below the resonance being investigated. This contribution to the instrumental tail must be due to protons which are degraded in energy either by having penetrated the edge of one of the beam defining slits, or by Rutherford scattering in the target or target backing followed by capture. These peaks are best observed in the spectra of relatively weak resonances at rather low proton energy, e.g. at $E_p = 609$ and 656 keV.

Finally direct capture has to be taken into account. The formalism for the calculation of the corresponding cross-sections has been worked out by Rolfs ⁷⁾. The final-state spectroscopic factors which enter into the calculation were taken from the $^{25}\text{Mg}(\tau, d)^{26}\text{Al}$ measurements of ref. ⁸⁾. The largest cross-sections are found for final states with $l_p(\tau, d) = 0$. For instance, for the $E_x = 0.42$ MeV $J^\pi = 3^+$ level (with $C^2S = 0.51$ for $l_p = 0$, $C^2S = 0.26$ for $l_p = 2$) the $l_p = 0$ contribution dominates over $l_p = 2$ by a factor of 9 at $E_p = 1.5$ MeV. The $E_x = 0.42$ MeV cross-section dominates over those for all other states by factors of at least 2. The interference between direct and resonant capture has not been considered.

If, after subtraction of all the possible contributions mentioned above (with errors assigned to them of at least 50%), a statistically significant intensity remains, it can be considered as due to a resonance primary. The process has eliminated all potential primaries of octupole or higher multipolarity, has severely reduced the number of M2 primaries (to about seven), and has also thrown out some E2 primaries. Examples of some weak transitions are given in table 3. To translate peak intensities into cross-sections, the expressions given by Gove ⁹⁾ have been used, both for the case that the target thickness exceeds the resonance width and vice versa. It is seen that for five out of the eight transitions listed the BW tail sum together with the direct capture contribution nicely explains the observed peak cross-sections, whereas for the other three an M2 primary remains after subtraction of these two contributions.

TABLE 3
Examples of weak primaries ^a

E_p	E_{xr}	E_{xf}	$J_r^\pi; T_r \rightarrow J_f^\pi; T_f$	b	σ_{exp}	BWTS	DC	Conclusion
	[keV]			[%]			[nb]	
685	6964 \rightarrow	0	$3^-; 1 \rightarrow 5^+; 0$	0.037 $\underline{6}$	128		4.0	b
811	7086 \rightarrow	417	$1^-; 1 \rightarrow 3^+; 0$	0.041 $\underline{10}$	44	3.5	34	c
896	7168 \rightarrow	1759	$4^-; 0 \rightarrow 2^+; 0$	0.19 $\underline{7}$	105	82	14	c
969	7238 \rightarrow	0	$3^-; 0 \rightarrow 5^+; 0$	0.16 $\underline{2}$	168	4	2.6	d
	\rightarrow 1058		$\rightarrow 1^+; 0$	0.09 $\underline{3}$	95		12	e
1680	7921 \rightarrow	417	$5^+; 0 \rightarrow 3^+; 0$	7.4 $\underline{4}$	1400	865	690	c
	\rightarrow 1759		$\rightarrow 2^+; 0$	1.7 $\underline{5}$	315	115	240	c
	\rightarrow 3160		$\rightarrow 2^+; 1$	1.9 $\underline{2}$	355	45	330	c

^a Column 1 lists the resonance proton energy, columns 2 and 3 the excitation energies of the resonance and the final state, columns 4 and 5 their $J^\pi; T$ values, column 6 the branching of the transition, column 7 the corresponding cross-section (see text), column 8 the calculated Breit-Wigner tail sum, and column 9 the calculated contribution from direct capture. Possible coincident summing and instrumental tail contributions have already been subtracted.

^b An M2 transition remains of 0.14 $\underline{4}$ W.u.

^c The σ_{exp} is explained as the sum of BWTS and DC.

^d An M2 transition remains of 0.053 $\underline{9}$ W.u.

^e An M2 transition remains of 0.07 $\underline{3}$ W.u.

In table 4 the branchings are given of the $75\ ^{25}\text{Mg}(p, \gamma)^{26}\text{Al}$ resonances observed in the $E_p = 0.31\text{--}1.84$ MeV region. For reasons of space economy only the strong branches are listed ($b \geq 1\%$), in addition to those weak branches which are (also) instrumental in the determination of spins, parities and isospins. Furthermore errors have been rounded off to reduce the total entry to five symbols, such that e.g. 0.0971 $\underline{2}$ becomes 0.101 $\underline{1}$, and branching upper limits have been omitted for unobserved primaries. Finally, the $J^\pi; T$ values of resonances and final states had to be omitted; the resonance $J^\pi; T$ values are given in ref.¹⁾, those for bound states below $E_x = 6.0$ MeV in ref.¹⁶⁾, and those for the remaining levels in table 5. Branchings for the feeding of the levels at $E_x = 3822, 3978, 4480$ and 5462 MeV and of levels above $E_x = 6.0$ MeV are also given in table 5, to be discussed below. The total number of observed primaries (with weak transitions included) amounts to about 2200, with an average number per resonance of 29 and a maximum number (at the $E_p = 1237$ keV resonance) of 48.

Some special remarks should be made about the disentangling of the spectra of resonance doublets. An easy case, for instance, is the $E_p = 1370 + 1375$ keV doublet. Both resonances are narrow, such that the spectrum at $E_p = 1370$ keV does not show

TABLE 4

Resonance branchings (in %); all energies in keV, E_p underlined ^a

<u>317;</u>	6610	->	417	<u>331</u>	,	->	1759	15.8 <u>5</u> ,	->	2069	5.72	,	->	2545	1.38 <u>8</u> ,	->	2913	3.0 <u>1</u>	,		
		->	3160	11.4 <u>4</u> ,	->	3596	4.2 <u>2</u>	,	->	4192	18.7 <u>6</u> ,	->	4548	1.13 <u>6</u> ,	->	4940	0.09 <u>2</u> ,				
		->	5396	0.23 <u>3</u> ,	->	5726	0.08 <u>2</u>														
<u>390;</u>	6680	->	228	0.84 <u>6</u> ,	->	417	6.5 <u>3</u>	,	->	1058	2.0 <u>1</u>	,	->	1851	4.5 <u>2</u>	,	->	2070	18.2 <u>6</u> ,		
		->	2661	0.99 <u>6</u> ,	->	3160	5.6 <u>2</u>	,	->	4192	29.3 <u>9</u> ,	->	4548	3.0 <u>2</u>	,	->	4599	21.3 <u>7</u> ,			
		->	5132	0.07 <u>3</u> ,	->	5495	0.07 <u>2</u> ,	->	5545	3.6 <u>2</u>											
<u>435;</u>	6724	->	0	50 <u>1</u>	,	->	417	29.9 <u>2</u> ,	->	2545	1.60 <u>7</u> ,	->	4192	6.4 <u>2</u>	,	->	4599	5.3 <u>2</u>	,		
		->	4705	4.1 <u>1</u>	,	->	4952	0.064 <u>7</u> ,	->	5007	0.017 <u>4</u> ,	->	5676	0.034 <u>4</u> ,	->	5692	0.019 <u>4</u> ,				
		->	5916	0.024 <u>4</u>																	
<u>497;</u>	6784	->	417	2.0 <u>1</u>	,	->	1759	13.1 <u>4</u> ,	->	2070	15 <u>1</u>	,	->	2072	5.91 <u>0</u> ,	->	2365	2.26 <u>8</u> ,			
		->	2545	1.13 <u>5</u> ,	->	2913	4.0 <u>1</u>	,	->	3074	9.7 <u>3</u>	,	->	3160	26.2 <u>2</u> ,	->	4192	6.2 <u>2</u>	,		
		->	4548	7.5 <u>3</u>	,	->	4622	1.03 <u>5</u> ,	->	5457	0.60 <u>3</u>										
<u>503;</u>	6789	->	417	49.9 <u>8</u>	,	->	1759	16.8 <u>6</u> ,	->	2069	2.3 <u>1</u>	,	->	3160	5.8 <u>2</u>	,	->	3596	1.33 <u>8</u> ,		
		->	3681	3.2 <u>1</u>	,	->	4192	3.5 <u>1</u>	,	->	4548	1.01 <u>6</u> ,	->	4705	10.7 <u>4</u> ,	->	4940	0.48 <u>5</u> ,			
		->	5396	0.65 <u>5</u>																	
<u>515;</u>	6801	->	1759	9 <u>3</u>	,	->	2070	16 <u>3</u>	,	->	2365	1.8 <u>3</u>	,	->	2545	1.2 <u>3</u>	,	->	2661	4 <u>2</u>	,
		->	2913	3 <u>2</u>	,	->	3160	24 <u>4</u>	,	->	3681	3.0 <u>6</u>	,	->	3724	1.0 <u>4</u>	,	->	3963	1.4 <u>6</u>	,
		->	4192	5 <u>1</u>	,	->	4548	11 <u>2</u>	,	->	4599	11 <u>2</u>	,	->	4705	3.6 <u>8</u>	,	->	5545	1.1 <u>2</u>	,
		->	5924	0.6 <u>2</u>																	
<u>516;</u>	6802	->	1058	9 <u>3</u>	,	->	1759	221 <u>0</u>	,	->	1851	5 <u>2</u>	,	->	2072	11 <u>3</u>	,	->	2661	14 <u>5</u>	,
		->	2740	2.6 <u>8</u>	,	->	2913	10 <u>3</u>	,	->	3160	19 <u>6</u>	,	->	3724	4.4 <u>2</u>	,	->	3751	1.2 <u>5</u>	,
		->	5495	1.2 <u>5</u>																	
<u>533;</u>	6818	->	417	15.3 <u>6</u> ,	->	2069	2.2 <u>2</u>	,	->	2365	19.9 <u>7</u> ,	->	2545	43 <u>1</u>	,	->	3074	2.3 <u>2</u>	,		
		->	3403	1.99 <u>8</u> ,	->	3596	3.0 <u>2</u>	,	->	3675	2.0 <u>2</u>	,	->	3963	4.6 <u>2</u>	,	->	4548	0.46 <u>4</u> ,		
		->	4941	2.4 <u>2</u>	,	->	5142	0.09 <u>2</u> ,	->	5488	0.31 <u>4</u>										
<u>567;</u>	6852	->	228	0.15 <u>1</u> ,	->	417	32 <u>1</u>	,	->	1759	6.7 <u>2</u>	,	->	1851	1.1 <u>1</u>	,	->	2070	2.1 <u>2</u>	,	
		->	2072	6.7 <u>3</u>	,	->	2545	21.8 <u>6</u> ,	->	2913	6.6 <u>2</u>	,	->	3160	2.17 <u>7</u> ,	->	3596	6.6 <u>2</u>	,		
		->	4349	4.8 <u>2</u>	,	->	4548	2.09 <u>7</u> ,	->	4952	1.52 <u>5</u> ,	->	5598	0.03 <u>1</u>							
<u>591;</u>	6874	->	228	18.8 <u>8</u> ,	->	417	1.3 <u>5</u>	,	->	1759	1.4 <u>2</u>	,	->	1851	2.5 <u>2</u>	,	->	2070	44 <u>1</u>	,	
		->	3160	5.3 <u>2</u>	,	->	3754	14.2 <u>6</u> ,	->	4548	3.3 <u>2</u>	,	->	5142	1.09 <u>7</u> ,	->	5195	5.4 <u>2</u>			
<u>593;</u>	6876	->	228	0.221 <u>0</u> ,	->	417	29.3 <u>8</u> ,	->	1759	8.9 <u>3</u>	,	->	1851	2.01 <u>8</u> ,	->	2069	0.17 <u>3</u> ,				
		->	2072	6.9 <u>2</u>	,	->	2545	24.4 <u>7</u> ,	->	2913	6.1 <u>2</u>	,	->	3047	1.12 <u>5</u> ,	->	3160	1.90 <u>8</u> ,			
		->	3596	7.3 <u>2</u>	,	->	4349	4.4 <u>1</u>	,	->	4952	1.48 <u>5</u>									
<u>609;</u>	6892	->	0	28 <u>1</u>	,	->	3403	13.5 <u>6</u> ,	->	3508	3.0 <u>2</u>	,	->	4941	3.6 <u>2</u>	,	->	5396	47 <u>2</u>	,	
		->	5488	2.2 <u>3</u>	,	->	6084	2.3 <u>1</u>													
<u>656;</u>	6936	->	228	5.7 <u>2</u>	,	->	1058	22.2 <u>7</u> ,	->	1759	19.4 <u>6</u> ,	->	2070	5.9 <u>5</u>	,	->	2072	3.4 <u>5</u>	,		
		->	2365	0.19 <u>6</u> ,	->	2661	3.7 <u>2</u>	,	->	2913	2.5 <u>1</u>	,	->	3160	14.2 <u>5</u> ,	->	3751	3.3 <u>3</u>	,		
		->	3754	1.3 <u>4</u>	,	->	5142	11.7 <u>4</u> ,	->	6028	3.2 <u>1</u>										
<u>685;</u>	6964	->	417	35 <u>1</u>	,	->	1759	29.9 <u>2</u> ,	->	2069	1.63 <u>6</u> ,	->	2661	2.72 <u>2</u> ,	->	3074	1.05 <u>4</u> ,				
		->	3160	1.02 <u>4</u> ,	->	3596	1.65 <u>6</u> ,	->	3675	1.27 <u>4</u> ,	->	3681	7.1 <u>2</u>	,	->	5396	5.9 <u>2</u>	,			
		->	5457	0.73 <u>5</u> ,	->	5598	0.24 <u>1</u> ,	->	5676	6.4 <u>2</u>	,	->	5916	0.98 <u>3</u>							

1019;	7286	->	1851	563 ,	->	2072	62 ,	->	2740	92 ,	->	4622	1.04 ,	->	5007	1.46 ,
		->	6028	262												
1025;	7291	->	0	57.36,	->	417	2.062,	->	1759	4.02 ,	->	3681	1.084,	->	3751	4.31 ,
		->	4192	1.475,	->	4599	13.14,	->	4705	2.81 ,	->	5132	11.03			
1043;	7308	->	228	0.081,	->	417	30.54,	->	1058	5.92 ,	->	1759	4.32 ,	->	1851	1.225,
		->	2072	10.13,	->	2365	3.21 ,	->	2545	2.046,	->	2661	6.22 ,	->	2740	5.52 ,
		->	2913	12.54,	->	3596	8.53 ,	->	3681	1.445,	->	3724	1.705,	->	3751	2.417,
		->	5195	0.0184,	->	5457	0.052,	->	5585	1.535,	->	5692	0.062			
1084;	7348	->	0	18.46,	->	417	381 ,	->	2365	12.94,	->	2545	3.41 ,	->	3074	1.81 ,
		->	3596	2.61 ,	->	3681	4.31 ,	->	4192	3.61 ,	->	4431	0.443,	->	4705	1.505,
		->	5457	0.974,	->	5692	4.34 ,	->	6084	4.22						
1103;	7366	->	0	4.72 ,	->	417	6.72 ,	->	2069	3.31 ,	->	2545	1.265,	->	3596	1.595,
		->	3963	1.045,	->	4349	3.31 ,	->	4705	7.72 ,	->	5132	66.74,	->	5726	0.694
1135;	7397	->	417	181 ,	->	1759	1.45 ,	->	1851	2.81 ,	->	2072	3.32 ,	->	2365	1.33 ,
		->	2545	1.682,	->	2740	1.288,	->	2913	3.82 ,	->	3160	29.92,	->	3596	2.53 ,
		->	3681	2.03 ,	->	3724	2.01 ,	->	4349	1.597,	->	4599	16.35,	->	4705	0.195,
		->	5950	0.172,	->	6028	6.92									
1137;	7399	->	417	381 ,	->	1759	18.66,	->	2069	2.31 ,	->	2661	6.82 ,	->	2913	3.21 ,
		->	3074	3.61 ,	->	3596	5.32 ,	->	3681	4.62 ,	->	4192	1.327,	->	5396	1.776,
		->	5457	7.13 ,	->	5916	0.944									
1148;	7410	->	0	16.95,	->	417	482 ,	->	2365	7.93 ,	->	3074	1.857,	->	3403	1.12 ,
		->	3596	1.967,	->	3681	3.11 ,	->	4705	1.094,	->	5007	0.243,	->	5396	0.294,
		->	5457	1.275,	->	5598	0.162,	->	5692	6.62 ,	->	6084	6.22			
1164;	7425	->	0	291 ,	->	2365	2.41 ,	->	2661	1.722,	->	2913	6.43 ,	->	4599	1.588,
		->	4705	3.41 ,	->	5132	491 ,	->	5569	0.103						
1179;	7440	->	1058	181 ,	->	1851	392 ,	->	2072	3.65 ,	->	2740	201 ,	->	5010	1.63 ,
		->	5585	10.05												
1184;	7444	->	228	311 ,	->	1058	1.11 ,	->	1759	2.32 ,	->	1851	8.64 ,	->	2070	4.93 ,
		->	2072	2.63 ,	->	2661	3.22 ,	->	2740	1.01 ,	->	3160	361 ,	->	4548	3.82 ,
		->	5457	0.052,	->	5545	1.007,	->	5692	0.104						
1196;	7455	->	228	2.41 ,	->	417	0.994,	->	1058	1.517,	->	1851	1.528,	->	2070	662 ,
		->	3160	24.07,	->	5195	0.783									
1205;	7464	->	0	0.0837,	->	417	1.846,	->	1759	5.92 ,	->	1851	0.181,	->	2070	8.43 ,
		->	2365	6.92 ,	->	2545	8.53 ,	->	2661	6.02 ,	->	3160	5.62 ,	->	3675	17.06,
		->	3681	2.372,	->	3751	1.455,	->	3963	2.782,	->	4206	14.56,	->	4705	2.418,
		->	4773	0.703,	->	4952	3.082,	->	5132	4.71 ,	->	5142	1.264,	->	5495	1.796
1237;	7495	->	417	7.53 ,	->	1058	0.0505,	->	1759	5.42 ,	->	2070	5.52 ,	->	2365	9.03 ,
		->	2545	9.93 ,	->	2661	5.22 ,	->	3074	1.013,	->	3160	4.72 ,	->	3675	14.74,
		->	3681	1.926,	->	3751	1.946,	->	3963	2.528,	->	4206	14.95,	->	4705	1.244,
		->	4773	1.033,	->	4952	3.71 ,	->	5132	2.592,	->	5142	0.813,	->	5495	2.177
1239;	7497	->	417	8.76 ,	->	1851	4.43 ,	->	2070	2.810,	->	2072	10.16,	->	2365	2.54 ,
		->	2661	3.33 ,	->	2740	5.03 ,	->	3160	401 ,	->	3596	1.92 ,	->	3751	1.32 ,
		->	4192	2.11 ,	->	4599	3.52 ,	->	4622	5.63 ,	->	5676	0.397,	->	5692	4.02
1273;	7529	->	0	6.77 ,	->	3403	5.94 ,	->	3508	2.33 ,	->	5396	432 ,	->	5676	351

TABLE 4 - continued

<u>1283</u> ;	7540	->	417	4.02 ,	->	1759	11.44 ,	->	1851	9.74 ,	->	2072	17.16 ,	->	2365	4.62 ,
		->	2661	4.82 ,	->	2740	14.46 ,	->	3724	2.61 ,	->	3751	2.02 ,	->	4349	1.91 ,
		->	4622	12.15 ,	->	4940	0.585 ,	->	5457	4.42 ,	->	5692	0.62			
<u>1292</u> ;	7548	->	0	5.87 ,	->	3403	10.77 ,	->	3508	0.72 ,	->	3675	412 ,	->	4773	5.64 ,
		->	5132	2.92 ,	->	5245	2.32 ,	->	5396	2.42 ,	->	5676	3.42 ,	->	5692	2.82 ,
		->	5726	8.85 ,	->	5924	10.77									
<u>1302</u> ;	7558	->	228	0.092 ,	->	1851	1.62 ,	->	2070	221 ,	->	2072	3.14 ,	->	2365	2.23 ,
		->	2740	1.72 ,	->	2913	1.516 ,	->	3160	551 ,	->	3596	1.61 ,	->	3675	0.103 ,
		->	4599	5.32												
<u>1306</u> ;	7561	->	228	1.104 ,	->	417	3.11 ,	->	1058	1.225 ,	->	1759	5.92 ,	->	1851	6.12 ,
		->	2072	17.77 ,	->	2365	22.67 ,	->	2545	11.34 ,	->	2661	2.852 ,	->	2740	4.22 ,
		->	3074	1.576 ,	->	3596	12.94 ,	->	3963	1.485 ,	->	4349	2.922 ,	->	5195	0.052
<u>1337</u> ;	7592	->	0	7.43 ,	->	1759	2.32 ,	->	2069	3.42 ,	->	2545	3.82 ,	->	2661	3.72 ,
		->	2913	221 ,	->	3403	1.11 ,	->	3675	4.32 ,	->	3681	1.41 ,	->	3751	2.41 ,
		->	4192	15.25 ,	->	4599	13.55 ,	->	4705	11.94 ,	->	5726	16.95 ,	->	5924	3.01
<u>1342</u> ;	7596	->	0	5.44 ,	->	2069	5.03 ,	->	2365	4.93 ,	->	2545	7.74 ,	->	3403	4.02 ,
		->	3508	0.236 ,	->	3751	0.083 ,	->	3963	1.31 ,	->	4206	3.02 ,	->	4705	22.77 ,
		->	4952	2.92 ,	->	5132	22.17 ,	->	5245	4.02 ,	->	5726	5.22 ,	->	5924	6.83
<u>1351</u> ;	7605	->	417	2.63 ,	->	1759	1.73 ,	->	1851	1.12 ,	->	2070	17.17 ,	->	2072	1.34 ,
		->	2365	12.86 ,	->	2545	10.65 ,	->	2740	5.73 ,	->	3074	1.82 ,	->	3160	1.42 ,
		->	3596	5.43 ,	->	3724	1.21 ,	->	4349	2.52 ,	->	4431	1.12 ,	->	4548	1.51 ,
		->	4622	16.36 ,	->	4940	1.11 ,	->	5457	1.91 ,	->	5545	1.91 ,	->	6028	1.192
<u>1370</u> ;	7623	->	228	241 ,	->	417	3.13 ,	->	2070	16.38 ,	->	2072	1.13 ,	->	2740	1.62 ,
		->	2913	2.42 ,	->	3160	291 ,	->	3751	1.63 ,	->	3754	1.93 ,	->	3963	1.93 ,
		->	4548	12.45												
<u>1375</u> ;	7628	->	0	6.12 ,	->	2069	4.41 ,	->	3403	1.615 ,	->	3508	5.42 ,	->	3675	7.93 ,
		->	4192	0.403 ,	->	4206	41.08 ,	->	4599	0.923 ,	->	4773	13.64 ,	->	4941	3.41 ,
		->	5245	10.33 ,	->	5513	1.102									
<u>1396</u> ;	7648	->	228	246 ,	->	417	256 ,	->	1058	144 ,	->	3160	73 ,	->	3751	52 ,
		->	4192	52 ,	->	4548	163 ,	->	4599	42						
<u>1515</u> ;	7762	->	417	13.76 ,	->	1759	1.22 ,	->	2070	5.74 ,	->	2365	1.72 ,	->	2913	3.13 ,
		->	3074	1.02 ,	->	3160	15.27 ,	->	3596	2.62 ,	->	3751	3.02 ,	->	3963	1.42 ,
		->	4192	301 ,	->	4206	1.22 ,	->	4548	5.73 ,	->	4599	2.72 ,	->	4622	0.81 ,
		->	5132	2.02 ,	->	5396	1.01 ,	->	5431	0.498 ,	->	5457	1.11 ,	->	5726	1.11
<u>1525</u> ;	7772	->	0	0.882 ,	->	417	3.92 ,	->	1058	0.818 ,	->	1759	3.42 ,	->	2069	3.82 ,
		->	2070	2.62 ,	->	2661	1.51 ,	->	2740	1.118 ,	->	2913	1.398 ,	->	3160	29.72 ,
		->	3724	1.007 ,	->	4192	11.44 ,	->	4548	1.298 ,	->	4599	16.36 ,	->	5132	5.02 ,
		->	5545	6.32 ,	->	5726	1.016									
<u>1526</u> ;	7773	->	2740	113 ,	->	3160	675 ,	->	4622	62 ,	->	5457	92 ,	->	5598	72
<u>1568</u> ;	7814	->	228	151 ,	->	417	5.06 ,	->	1058	2.24 ,	->	2070	1.62 ,	->	2072	1.72 ,
		->	2661	1.83 ,	->	2740	1.43 ,	->	2913	1.02 ,	->	3160	1.12 ,	->	3754	392 ,
		->	4192	1.33 ,	->	4548	17.97 ,	->	5142	2.02 ,	->	5195	3.83			

TABLE 4 - continued

<u>1580</u> ;	7825	->	0	161	,	->	417	251	,	->	2069	1.53	,	->	2545	1.12	,	->	3074	1.82	,
		->	3403	1.42	,	->	3596	2.43	,	->	4192	241	,	->	4206	1.12	,	->	4622	0.3612	,
		->	4705	5.84	,	->	4952	0.8015	,	->	5132	5.13	,	->	5396	1.02	,	->	5457	2.12	,
		->	5726	1.21																	
<u>1587</u> ;	7832	->	0	56.65	,	->	417	2.21	,	->	2365	2.61	,	->	3074	4.22	,	->	3508	0.071	,
		->	3751	1.215	,	->	4192	5.72	,	->	4599	6.62	,	->	4952	0.453	,	->	5132	10.13	,
		->	5726	1.345	,	->	5849	0.101													
<u>1622</u> ;	7865	->	417	331	,	->	1058	2.63	,	->	1759	3.95	,	->	1851	2.02	,	->	2070	19.18	,
		->	2365	1.22	,	->	2545	5.94	,	->	2661	3.33	,	->	2740	1.52	,	->	3074	1.22	,
		->	3160	1.23	,	->	3963	6.33	,	->	4599	4.12	,	->	4773	0.277	,	->	5142	4.02	,
		->	5545	3.32	,	->	6028	0.92													
<u>1632</u> ;	7874	->	1759	1.03	,	->	2069	121	,	->	2070	521	,	->	2545	1.41	,	->	2740	0.418	,
		->	3160	4.52	,	->	3751	1.81	,	->	4192	1.267	,	->	4548	8.03	,	->	4599	6.52	,
		->	5142	3.71	,	->	5396	0.185	,	->	5545	2.102									
<u>1637</u> ;	7880	->	2070	355	,	->	2072	325	,	->	2661	122	,	->	2913	2.18	,	->	3160	63	,
		->	3754	1.77	,	->	4192	1.26	,	->	4431	1.34	,	->	5545	1.47					
<u>1649</u> ;	7891	->	0	39.85	,	->	417	4.52	,	->	2069	3.11	,	->	2365	28.32	,	->	3074	5.72	,
		->	3160	0.102	,	->	3675	1.537	,	->	3681	1.377	,	->	4206	4.51	,	->	4349	1.325	,
		->	4773	3.61	,	->	4952	2.802													
<u>1680</u> ;	7921	->	0	12.27	,	->	2069	6.910	,	->	3403	7.74	,	->	3508	5.63	,	->	4192	1.12	,
		->	4206	522	,	->	4773	3.32	,	->	4941	2.14	,	->	5513	1.21	,	->	5569	1.11	
<u>1699</u> ;	7939	->	0	0.101	,	->	417	4.72	,	->	2069	69.25	,	->	2070	1.63	,	->	2365	3.01	,
		->	2545	5.52	,	->	2661	2.572	,	->	3751	2.902	,	->	3963	2.408	,	->	4773	1.114	
<u>1714</u> ;	7953																				
<u>1744</u> ;	7982	->	417	41.57	,	->	1058	4.52	,	->	1759	7.02	,	->	1851	7.73	,	->	2072	1.32	,
		->	2545	9.13	,	->	2661	4.02	,	->	2740	1.338	,	->	2913	1.922	,	->	3074	1.942	,
		->	3681	1.487	,	->	3724	3.31	,	->	3754	0.147	,	->	3963	6.12	,	->	4349	1.055	,
		->	5883	1.998																	
<u>1763</u> ;	8001	->	228	5.53	,	->	1058	10.34	,	->	2072	1.93	,	->	2661	5.32	,	->	2740	1.82	,
		->	3160	1.52	,	->	3724	4.02	,	->	4431	9.74	,	->	4548	1.32	,	->	4622	2.12	,
		->	4940	13.24	,	->	5007	3.42	,	->	5692	0.184									
<u>1771</u> ;	8008	->	417	22.07	,	->	1759	3.21	,	->	1851	2.21	,	->	2070	18.86	,	->	2545	2.81	,
		->	2661	3.71	,	->	3160	1.256	,	->	3675	0.155	,	->	3724	1.386	,	->	3963	4.21	,
		->	4192	2.098	,	->	4548	20.86	,	->	4599	5.72	,	->	5142	1.727	,	->	5950	0.052	,
		->	6028	1.616																	
<u>1774</u> ;	8011	->	0	2.82	,	->	2069	8.85	,	->	3403	2.82	,	->	3508	7.23	,	->	3675	301	,
		->	4705	2.31	,	->	4773	3.92	,	->	5132	1.172	,	->	5396	10.64	,	->	5676	16.76	,
		->	5726	2.71	,	->	6048	4.02													
<u>1800</u> ;	8036	->	228	8.814	,	->	1058	132	,	->	1759	6.113	,	->	1851	5.713	,	->	2070	4.313	,
		->	2072	5.713	,	->	2661	3.27	,	->	2913	3.78	,	->	3160	7.310	,	->	3724	2.97	,
		->	3751	2.911	,	->	3754	8.82	,	->	4431	4.42	,	->	4548	7.02	,	->	4622	1.25	,
		->	4940	5.17	,	->	5195	3.36	,	->	5545	1.66	,	->	5849	1.83					

TABLE 4 - continued

<u>1811</u> ; 8047	-> 417	7.9 <u>4</u> , -> 1759	1.2 <u>1</u> , -> 2069	5.0 <u>6</u> , -> 2070	2.7 <u>6</u> , -> 2365	4.8 <u>3</u> ,
	-> 2545	6.8 <u>3</u> , -> 2661	2.2 <u>2</u> , -> 2913	3.4 <u>5</u> , -> 3160	5.2 <u>2</u> , -> 3681	4.6 <u>2</u> ,
	-> 3963	1.3 <u>1</u> , -> 4192	10.5 <u>4</u> , -> 4349	1.13 <u>9</u> , -> 4431	1.1 <u>2</u> , -> 4548	7.0 <u>3</u> ,
	-> 4599	14.7 <u>5</u> , -> 5132	2.0 <u>1</u> , -> 5545	4.3 <u>2</u> , -> 5883	2.6 <u>1</u> , -> 5924	1.3 <u>5</u> ,
	-> 5950	0.12 <u>5</u>				
<u>1829</u> ; 8064	-> 228	0.45 <u>6</u> , -> 417	51 <u>1</u> , -> 2072	1.1 <u>1</u> , -> 2365	1.3 <u>1</u> , -> 2661	8.4 <u>3</u> ,
	-> 2740	2.2 <u>1</u> , -> 2913	2.9 <u>2</u> , -> 3675	0.16 <u>7</u> , -> 3754	0.19 <u>7</u> , -> 3963	12.4 <u>4</u> ,
	-> 5883	10.0 <u>4</u>				
<u>1833</u> ; 8067	-> 0	36.3 <u>7</u> , -> 2069	1.2 <u>2</u> , -> 3403	1.21 <u>7</u> , -> 3508	2.2 <u>1</u> , -> 3675	14.0 <u>6</u> ,
	-> 4773	1.39 <u>7</u> , -> 5396	11.5 <u>4</u> , -> 5676	18.5 <u>4</u> , -> 5924	0.16 <u>4</u> , -> 6084	5.8 <u>2</u>

^a Only the strong branches are listed ($b > 1\%$) with, in addition, those weak branches which are (also) instrumental in $J^\pi; T$ determinations. For branches to the $E_x = 3922$, 3978, 4480 and 5462 keV levels and to the levels above $E_x = 6.0$ MeV, see table 5; for the $E_p = 1714$ keV resonance, see table 1.

TABLE 5

Feeding of some weakly excited ^{26}Al secondary states including all levels above $E_x = 6.0$ MeV ($E_{xf}[\text{keV}]$, $J^\pi_f; T_f$, $E_p[\text{keV}]$, $b[\%]$) ^a

3922	$7^+(5^+); 0$	609 0.11 <u>5</u> , 738 0.20 <u>3</u> , 1273 0.401 <u>5</u> , 1375 0.023 <u>9</u> , 1680 2.3 <u>2</u>	
3978	$0^-; 0$	516 0.471 <u>5</u> , 656 0.08 <u>3</u> , 811 0.06 <u>2</u> , 1184 0.15 <u>4</u> , 1763 22.8 <u>7</u>	b
4480	$0^-; 0$	497 0.70 <u>4</u> , 811 4.181 <u>3</u> , 1184 0.14 <u>3</u> , 1239 0.45 <u>7</u> , 1637 1.1 <u>3</u>	c
5462	$0^+(1,2); 0$	1637 1.1 <u>3</u> , 1763 1.27 <u>7</u> , 1771 0.11 <u>3</u>	
6028	$1^+(1^-); 1$	5 branchings $> 1\%$ given in table 4	d
6084	$5^+; 0$	7 branchings $> 1\%$ given in table 4	d
6086	$1^-(2^+); 0$	723 0.040 <u>7</u> , 811 0.14 <u>1</u> , 890 0.11 <u>3</u> , 986 0.05 <u>2</u> , 1283 0.76 <u>5</u>	e
6120	$(4,5^+); 0$	953 0.88 <u>3</u> , 1342 0.22 <u>5</u> , 1375 1.47 <u>5</u> , 1632 0.12 <u>3</u> , 1774 0.75 <u>9</u>	f
6198	$1(2^+); 0$	811 0.028 <u>9</u> , 1043 0.019 <u>5</u> , 1179 5.11 <u>3</u> , 1342 0.05 <u>3</u> , 1714 0.007 <u>2</u>	g
6238	$1; 0$	656 0.05 <u>2</u> , 811 0.046 <u>6</u> , 819 0.34 <u>8</u> , 1351 0.32 <u>8</u> , 1763 8.9 <u>4</u>	h
6254	$3^-; 0$	533 0.05 <u>1</u> , 969 0.05 <u>1</u> , 1205 0.020 <u>4</u> , 1744 0.06 <u>3</u> , 1829 0.34 <u>5</u>	i
6270	$1; 0$	811 0.06 <u>2</u> , 1306 0.30 <u>1</u> , 1351 0.12 <u>6</u> , 1744 0.39 <u>8</u> , 1763 0.07 <u>5</u>	j
6280	$3^+; 0$	weakly excited at 13 resonances	
6343	$4^-; 0$	953 0.42 <u>1</u> , 1137 0.032 <u>9</u> , 1375 1.18 <u>4</u> , 1649 0.09 <u>3</u> , 1699 0.66 <u>2</u>	k
6364	$3^+; 1$	excited at 22 resonances	
6399	$2^-; 0$	811 0.019 <u>5</u> , 986 0.136 <u>2</u> , 1184 0.10 <u>3</u> , 1205 0.031 <u>4</u> , 1239 0.29 <u>6</u>	l
6414	$0^+; 1$	928 0.068 <u>7</u> , 1184 0.09 <u>3</u> , 1196 0.023 <u>6</u> , 1370 0.84 <u>8</u> , 1763 0.16 <u>4</u>	
6436	$4^-; 0$	953 0.014 <u>3</u> , 1273 0.851 <u>2</u> , 1337 0.18 <u>3</u> , 1587 0.06 <u>1</u> , 1649 0.052 <u>8</u>	m
6426	$5^+(4^+); 0$	953 0.045 <u>4</u> , 1375 0.05 <u>1</u> , 1587 0.06 <u>3</u> , 1680 0.991 <u>0</u> , 1714 0.249 <u>8</u>	
6551	$4^+(5^+); 0$	1084 0.17 <u>2</u> , 1148 0.32 <u>1</u> , 1714 0.015 <u>5</u>	
6528	$(4,5^+); 0$	953 0.005 <u>2</u> , 1273 0.06 <u>2</u> , 1649 0.04 <u>1</u> , 1714 0.026 <u>3</u>	

TABLE 5 - continued

<u>6610</u>	$3^-;0$	1148 0.013 <u>5</u> , 1237 0.020 <u>4</u> , 1306 0.023 <u>6</u> , 1351 0.35 <u>7</u> , 1649 0.019 <u>6</u>
<u>6680</u>	$2^+;0$	986 0.027 <u>6</u> , 1205 0.06 <u>2</u> , 1237 0.152 <u>6</u> , 1306 0.57 <u>2</u> , 1699 0.097 <u>2</u> ⁿ
<u>6724</u>	$4^-;0$	1137 0.28 <u>3</u> , 1148 0.011 <u>5</u> , 1649 0.019 <u>6</u> , 1714 0.007 <u>2</u> , 1774 0.18 <u>6</u>
<u>6784</u>	$2^-;0$	1184 0.17 <u>7</u>
<u>6789</u>	$3^-;0$	1699 0.024 <u>8</u>
<u>6801</u>	$3^+;0$	1237 0.018 <u>4</u> , 1306 0.023 <u>6</u> , 1714 0.010 <u>2</u>
<u>6802</u>	$1(2^-);1$	1196 0.11 <u>1</u> , 1302 0.18 <u>1</u> , 1351 0.18 <u>6</u> , 1771 0.21 <u>3</u>
<u>6816</u>	$6^+(4,5);0$	1375 0.25 <u>6</u> , 1774 0.30 <u>5</u> , 1833 0.20 <u>3</u>
<u>6818</u>	$4^+;1$	1103 0.13 <u>2</u> , 1205 0.124 <u>6</u> , 1237 0.081 <u>6</u> , 1292 0.37 <u>7</u> , 1337 0.08 <u>2</u> ^o
<u>6852</u>	$2^+;1(+0)$	969 0.06 <u>1</u> , 1351 0.22 <u>6</u> , 1370 0.20 <u>4</u> , 1525 0.51 <u>6</u> , 1568 1.0 <u>5</u> ^p
<u>6874</u>	$1^+;0$	1829 0.501 <u>0</u>
<u>6876</u>	$2^+;1$	1351 0.20 <u>5</u> , 1525 0.33 <u>3</u> , 1632 0.09 <u>3</u>
<u>6892</u>	$6^-;0$	1292 0.25 <u>9</u> , 1375 0.021 <u>3</u> , 1774 4.5 <u>2</u> , 1833 5.1 <u>2</u>
<u>6964</u>	$3^-;1$	1351 0.701 <u>0</u> , 1515 0.43 <u>7</u> , 1525 0.23 <u>3</u> , 1580 1.711 <u>4</u>
<u>7001</u>	$2^+;0$	1699 0.036 <u>6</u>
<u>7015</u>	$5^+;0$	1714 0.025 <u>3</u> , 1833 0.37 <u>6</u>
<u>7109</u>	$4^-;0$	1714 0.102 <u>4</u>
<u>7222</u>	$5^+;1$	1273 0.6 <u>2</u> , 1680 1.141 <u>0</u>
<u>7291</u>	$4^+(3^+);0$	1714 0.062 <u>3</u>
<u>7348</u>	$4^-;1+0$	1680 0.701 <u>0</u>

^a Underlined levels have been seen as resonances (dashed line from ref. ¹⁰), solid line from present work). The $J^\pi;T$ values are to be discussed in a succeeding paper. ^b In addition: 1800 6.39. ^c In addition: 1763 0.225.

^d Also weakly excited at another seven resonances.

^e In addition: 1302 0.0245, 1351 0.988, 1568 0.4210, 1763 0.436.

^f In addition: 1833 0.336. ^g In addition: 1744 0.052, 1763 0.234.

^h In addition: 1829 0.73. ⁱ In addition: 1833 0.112. ^j In addition: 1771 0.062.

^k In addition: 1714 0.0186. ^l In addition: 1699 0.00449. ^m In addition: 1714 0.2017.

ⁿ In addition: 1744 0.443, 1763 0.134, 1829 0.798.

^o In addition: 1587 0.143, 1632 0.313. ^p In addition: 1632 0.203, 1771 0.103.

any contribution from the $E_p = 1375$ keV resonance. The spectrum at $E_p = 1375$ keV does contain a contribution from the lower-energy resonance through its instrumental tail, but the corresponding primaries are shifted down in energy by 4.8 keV, and furthermore the $J^\pi;T$ values are very different ($1^+;0$ and $5^+;1$, respectively). Consequently the $E_p = 1370$ keV decay contains a few primaries, like the 24% branch to the $E_x = 0.23$ MeV $0^+;1$ level, which impossibly could originate from the $E_p = 1375$ keV decay, such that the instrumental tail in the $E_p = 1375$ keV spectrum can be subtracted accurately.

The problem becomes much harder if the resonances are very close, or if one component (or both components) is (are) broad, in which case the primary γ -ray

energy is of little use. We now have to rely completely on the “signature” transitions (of which an example has been given above), transitions which can occur in the decay of one resonance but not in that of the other. At the $E_p = 1135 + 1137$ keV doublet, for instance, with $J^\pi; T = 2^+; 0$ and $3^-; 1$, respectively, there are five primaries to $J^\pi = 1^+$ levels which can only originate from the lower and three transitions to 4^- levels which can only originate from the upper component, and which together fix the two coefficients determining the amounts of interpenetration of the two spectra. The intensities of the primaries to a particular $J = 2$ or $J = 3$ level (and to 1^- and 4^+ levels) can then be found by solving two linear equations with two unknowns.

The branchings given by De Neys *et al.*²⁾ for 44 resonances are in very good overall agreement with the present results. Because they used an unshielded detector, their detection limit for weak transitions (especially of low energy) is higher by up to two orders of magnitude. The many weak transitions which thus remained unobserved cause their branchings for strong primaries to be high by about 5%. At $E_p = 593, 1137$ and 1237 keV a comparison makes no sense because these resonances turned out to be doublets, and at $E_p = 819$ and 1306 keV the subtraction of the contribution of the preceding resonance ($E_p = 811$ and 1302 keV, respectively) introduced errors. Also the decay to doublet levels (e.g. those at $E_x = 3.68$ and 3.75 MeV) has caused difficulties, and finally the many single- and double-escape peaks have not always been recognized as such. The decay of the $E_p = 1196$ keV resonance has also been studied by Keinonen *et al.*¹³⁾, who observed 12 primaries as against 8 in ref.²⁾ and 22 in the present work.

Most bound states are excited at many resonances; the proton binding energy is at $E_x = 6306.0(5)$ keV [ref.¹⁷⁾]. Of the levels below $E_x = 6.2$ MeV there are only four, either with very high spin ($E_x = 3922$ keV), or with very low spin ($E_x = 3978, 4480$ and 5462 keV), which are excited at less than seven resonances. The resonances at which they are excited, with the corresponding branchings, are listed in table 5, which also gives the feeding of the secondary states above $E_x = 6.0$ MeV. All the listed levels above $E_x = 6.45$ MeV have been seen as resonances (but for the level at $E_x = 6816$ keV which probably has $J^\pi = 6^+$), as reported in ref.¹⁰⁾ for the lowest three, and in ref.¹⁾ for the others. They are excited by altogether 74 resonance \rightarrow resonance transitions. All 15 known resonances below $E_x = 6.90$ MeV ($E_p = 0.62$ MeV) are excited in such transitions. None of the transitions listed in table 5 (but for the 4% branch to $E_x = 4480$ keV at $E_p = 811$ keV) has been given in ref.²⁾.

In the next two sections the branchings of secondary states and the resonance branchings will be discussed, respectively. Actually the determinations of these two sets of branchings are closely connected, due to the frequent occurrence of composite peaks, and to the restrictions on intensities imposed by the intensity balances at secondary levels. As the resonance spectra were analysed, one after the other, new secondary-state decay lines were observed and correspondingly the secondary-state branchings were gradually improved. Then, from the final set of resonance spectra,

the spectra were selected which gave the best statistics for the decay of a particular secondary state, and the branchings obtained were properly averaged. For a low-lying level (excited by several bound \rightarrow bound transitions, in addition to the primary) the easiest procedure for averaging is first to calculate the relative intensities of all decay lines with respect to a strong decay line which is uncontaminated in all spectra, then to average, and finally to divide by the sum of all ratios. If I_{in} (not used in the above procedure) systematically exceeds I_{out} , this formed an incentive to search for unspotted decay lines. For high-lying levels, only excited by an uncontaminated primary, and especially for levels of which the decay is split up in many weak lines, it is best to derive the branchings directly as the ratios of those lines relative to the primary.

The much improved secondary-state branchings thus obtained were then used to reanalyse all resonance spectra. The component intensities of composite peaks could now be determined with more confidence, which resulted in better resonance branchings and secondary-state intensity balances. It should be noted that the analysis of composite peaks in the $\theta = 55^\circ$ spectra is more difficult than for the γ -spectra accompanying e.g. beta-decay or thermal neutron capture, because Doppler patterns differ according to the lifetime of the upper level.

The procedure described above shows that the determination of (p, γ) branchings is an iterative process in which the branchings of resonances and of secondary states are closely interrelated.

One may wonder whether $\gamma\gamma$ -coincidence measurements would not also have been advantageous for obtaining secondary-state branchings. We are convinced, however, that the present method (singles spectra with good statistics at many resonances) is superior, and certainly far less time consuming. The disadvantage of the appearance of composite peaks in the singles spectra and the problem of the placement of "new" lines is far more than offset by the possibility to compare the spectra taken at several resonances where usually the component intensities in such peaks are very different.

4. Branchings of secondary states; previously unobserved levels

The branchings of secondary states derived from the CSS spectra taken at 55° are given in table 6. The decay of resonances is not included, but for those at $E_x = 6496, 6551$ and 6598 keV which were observed as very weak resonances by Elix *et al.*¹⁰⁾. For branching errors, see sect. 3. The table contains 548 entries, about four times as many as in the last $A = 26$ compilation¹¹⁾, with a maximum of 20 branches for the $E_x = 5245$ keV level. Part of the decay of three high-energy weakly excited levels is probably missing, because I_{in} exceeds I_{out} by more than twice the combined error; of the $E_x = 6254$ and 6399 keV levels not a single decay branch has been observed.

TABLE 6
Branchings (in %) of ^{26}Al secondary states (E_x in keV) ^a

<u>417</u>	→	0 100	A
<u>1058</u>	→	228 100	A
<u>1759</u>	→	417 98.01, → 1058 2.036	A
<u>1851</u>	→	228 99.32, → 417 0.679	B
<u>2069</u>	→	0 311, → 417 691	A
<u>2070</u>	→	228 3.04, → 417 21.48, → 1058 75.42, → 1759 0.172, → 1851 0.041	A
<u>2072</u>	→	228 89.42, → 417 10.62, → 1851 0.041	A
<u>2365</u>	→	0 0.894, → 417 331, → 1058 13.74, → 1759 1.485, → 2070 511	A
<u>2545</u>	→	0 0.216, → 417 261, → 1058 2.52, → 1759 3.32, → 2070 681	A
<u>2661</u>	→	417 612, → 1058 9.03, → 1759 0.625, → 1851 1.52, → 2070 251, → 2072 3.48	B
<u>2740</u>	→	228 99.22, → 417 0.82	C
<u>2913</u>	→	417 29.69, → 1058 0.794, → 1759 0.794, → 1851 1.054, → 2070 67.82	B
<u>3074</u>	→	0 0.792, → 417 0.52, → 1058 12.34, → 1759 0.374, → 1851 2.698, → 2070 83.45	B
<u>3160</u>	→	see table 8	B
<u>3403</u>	→	0 371, → 417 571, → 2069 5.32, → 2365 0.486	B
<u>3508</u>	→	0 99.71, → 2069 0.327	B
<u>3596</u>	→	0 3.72, → 417 0.184, → 1058 3.21, → 1851 0.986, → 2070 92.02	B
<u>3675</u>	→	0 4.42, → 417 57.12, → 1759 27.48, → 2069 1.01, → 2365 8.14, → 2545 2.02	B
<u>3681</u>	→	0 0.727, → 417 1.657, → 1058 2.62, → 1759 1.156, → 1851 0.184, → 2070 93.32, → 2913 0.125, → 3160 0.264	B
<u>3724</u>	→	228 99.21, → 1058 0.442, → 2661 0.352	C
<u>3751</u>	→	417 6.28, → 1058 9.63, → 1759 0.196, → 1851 0.277, → 2070 692, → 2365 0.137, → 2913 0.397, → 3160 161	C
<u>3754</u>	→	1058 86.04, → 1851 2.63, → 2072 9.52, → 2740 1.92	C
<u>3922</u>	→	0 100	F
<u>3963</u>	→	0 5.53, → 417 3.93, → 1058 11.14, → 1759 2.23, → 1851 1.62, → 2070 701, → 2365 3.43, → 2661 1.57, → 2740 0.52	C
<u>3978</u>	→	1058 371, → 1851 621, → 2072 0.92	C
<u>4192</u>	→	0 0.246, → 417 58.82, → 1759 3.92, → 2069 23.97, → 2365 9.35, → 2545 2.11, → 2661 0.52, → 2913 0.394, → 3596 0.887	B
<u>4206</u>	→	0 2.92, → 417 661, → 1759 1.107, → 2069 10.67, → 2365 6.85, → 2545 3.22, → 2661 8.15, → 2913 0.635, → 3074 0.523, → 3675 0.041	A
<u>4349</u>	→	0 0.61, → 417 2.66, → 1058 1.82, → 1759 0.802, → 2070 94.26	C
<u>4431</u>	→	417 293, → 1058 0.72, → 1759 2.96, → 1851 0.63, → 2070 613, → 2365 1.86, → 2545 1.03, → 3160 3.53	D
<u>4480</u>	→	1058 5.25, → 1851 341, → 2072 441, → 2740 16.36	C
<u>4548</u>	→	228 0.575, → 417 331, → 1058 481, → 1759 7.02, → 1851 0.083, → 2072 1.306, → 2365 3.31, → 2545 5.32, → 2661 0.205, → 2740 0.715, → 2913 0.484, → 3681 0.223	A
<u>4599</u>	→	417 25.38, → 1759 47.72, → 2069 2.61, → 2365 2.61, → 2545 5.02, → 2661 6.63, → 2913 3.42, → 3074 1.01, → 3675 3.12, → 3681 0.795, → 3751 1.82	C
<u>4622</u>	→	417 11.58, → 1058 1.53, → 1851 9.17, → 2072 18.38, → 2365 1.23, → 2545 2.16, → 2661 19.25, → 2740 321, → 3074 4.54, → 3160 1.12	D

TABLE 6 - continued

<u>5585</u>	->	228 86.47	, ->	1759 1.44	, ->	2913 2.63	, ->	3160 1.03	, ->	3754 2.43	, ->	4548 6.23	D
<u>5598</u>	->	417 293	, ->	2070 313	, ->	3160 403							E
<u>5671</u>	->	228 112	, ->	417 5.82	, ->	1058 7.812	, ->	3160 231	, ->	3681 3.28	, ->	3754 492	D
<u>5676</u>	->	0 401	, ->	417 451	, ->	2069 0.387	, ->	2365 0.798	, ->	2545 3.51	, ->	3675 0.228	B
	->	3681 1.368	, ->	4192 7.02	, ->	4599 1.608							
<u>5692</u>	->	417 441	, ->	1759 16.45	, ->	2070 0.318	, ->	2661 0.319	, ->	3074 0.699	, ->	3160 16.55	
	->	3596 0.296	, ->	3681 1.81	, ->	4192 18.36	, ->	4206 0.428	, ->	4548 0.212	, ->	4599 0.248	C
	->	5142 0.237											
<u>5726</u>	->	0 371	, ->	417 331	, ->	2069 6.03	, ->	2365 5.02	, ->	3403 81	, ->	3596 2.42	C
	->	3675 0.71	, ->	3963 6.13	, ->	4349 0.81							
<u>5849</u>	->	417 82	, ->	1759 72	, ->	2070 483	, ->	2740 3.22	, ->	2913 73	, ->	4192 152	E
	->	4548 8.42	, ->	5142 3.16									
<u>5883</u>	->	417 141	, ->	1759 3.112	, ->	1851 4.16	, ->	2070 11.67	, ->	3074 1.04	, ->	3160 9.37	
	->	4192 1.77	, ->	4548 432	, ->	4599 2.35	, ->	4622 3.17	, ->	4705 2.28	, ->	5132 2.210	D
	->	5142 2.310											
<u>5916</u>	->	417 442	, ->	1058 62	, ->	1759 6.65	, ->	1851 4.711	, ->	2070 21.47	, ->	2365 1.64	D
	->	2913 1.94	, ->	3160 3.34	, ->	3751 2.312	, ->	4192 6.44	, ->	5142 1.22			
<u>5924</u>	->	0 182	, ->	2069 112	, ->	2545 483	, ->	3403 3.56	, ->	3681 193			E
<u>5950</u>	^b ->	228 112	, ->	2070 173	, ->	3160 343	, ->	3754 162					F
<u>6028</u>	->	1058 442	, ->	1759 1.25	, ->	2072 2.96	, ->	2740 3.57	, ->	2913 15.45	, ->	3724 22.17	E
	->	3751 3.52	, ->	3978 0.93	, ->	4940 5.46	, ->	5007 1.12					
<u>6084</u>	->	0 15.15	, ->	2069 562	, ->	3508 7.83	, ->	3675 111	, ->	4705 8.94	, ->	4773 0.742	C
	->	5396 0.727											
<u>6086</u>	^b ->	228 296	, ->	1759 103	, ->	1851 186	, ->	2070 196					F
<u>6120</u>	->	2069 681	, ->	3403 261	, ->	3675 6.18							C
<u>6198</u>	->	228 100											F
<u>6238</u>	->	228 151	, ->	417 141	, ->	1058 2.36	, ->	1759 1.86	, ->	2070 281	, ->	2740 42	
	->	2913 1.24	, ->	3160 1.35	, ->	3724 0.53	, ->	3754 5.17	, ->	3978 72	, ->	4431 1.34	D
	->	4548 10.27	, ->	5142 7.87									
<u>6254</u>	no decay lines observed												F
<u>6270</u>	^b ->	228 583	, ->	3160 132	, ->	5195 52							E
<u>6280</u>	->	2070 94	, ->	3160 358	, ->	4192 234	, ->	4599 104	, ->	5132 105	, ->	5142 136	E
<u>6343</u>	->	2069 8.75	, ->	2365 3.85	, ->	2545 131	, ->	3074 5.111	, ->	4192 141	, ->	4599 462	D
	->	4705 3.810	, ->	5132 6.77									
<u>6364</u>	->	417 122	, ->	1759 273	, ->	2069 82	, ->	2365 82	, ->	2545 52	, ->	3675 124	E
	->	3681 131	, ->	3751 6.28	, ->	4192 1.511	, ->	4206 72					
<u>6399</u>	no decay lines observed												F
<u>6414</u>	->	1058 4010	, ->	1851 6010									F
<u>6436</u>	->	417 193	, ->	2069 72	, ->	4705 353	, ->	5132 394					F
<u>6496</u>	->	417 213	, ->	2365 191	, ->	2545 5.812	, ->	3403 4.52	, ->	4705 502			E
<u>6551</u>	^c ->	417 155	, ->	2069 133	, ->	2545 32	, ->	3403 32	, ->	3508 103	, ->	4206 62	F
	->	4705 115	, ->	4773 143	, ->	5132 203	, ->	5457 53					

TABLE 6 - continued

<u>6598</u>	<u>d</u> ->	<u>0 103</u>	, ->	<u>417 276</u>	, ->	<u>2365 53</u>	, ->	<u>2545 52</u>	, ->	<u>3681 43</u>	, ->	<u>4349 32</u>	,	
		->		<u>4705 467</u>										F
<u>6816</u>	->	<u>0 493</u>	, ->	<u>3675 513</u>										E

^a Initial state and errors are underlined. The last column gives an indication as to the quality of the decay data at the resonance where I_{out} is largest, with A standing for $I_{\text{out}} > 3000$, B 1000-3000, C 300-1000, D 100-300, E 30-100 and F < 30.

^b Decay incomplete.

^c Averages of present branchings with those reported by Elix et al. ¹⁰).

^d As reported by Elix et al. ¹⁰).

The statistical quality of the decay of a particular level, and thus the possibility to observe weak branches, naturally differs very much from level to level. For 27 levels the decay intensity at one or more resonances exceeds $I_{\text{out}} = 1000$ (for the definition of I , see table 2), for another 29 levels we have $I_{\text{out}} = 100-1000$, with $I_{\text{out}} < 100$ for the rest.

The possibility to obtain extensive and precise information on secondary-state branchings, as shown in table 6, is one of the particular advantages of the (p, γ) reaction as compared to, for instance, the (n, γ) reaction where good statistics can only be obtained at thermal energy. For the study of the decay of a particular level generally several (often many) resonances can be found where the level is strongly excited. A decay line which is contaminated at one resonance may be completely isolated at another. An example (for $E_x = 3.16$ MeV) is given below, where the decay of some secondary states is discussed, including all levels below $E_x = 3.2$ MeV.

1.76 MeV. The $1.76 \rightarrow 1.06$ MeV branching listed is the average of values obtained at five resonances. Statistics are best at $E_p = 685$ keV (fig. 3) where this 2% 701 keV line has a peak height of 3.9 times the underlying Compton continuum.

1.85 MeV. The new $E_\gamma = 1434$ keV $1.85 \rightarrow 0.42$ MeV branch coincides with the single-escape peak of the ever-present $E_\gamma = 1948$ keV $2.37 \rightarrow 0.42$ MeV transition. Statistics are best at $E_p = 811$ and 1306 keV.

The 2.07 MeV triplet. There are no resonances at which (through primary and/or secondary feeding) only a single component of the triplet is excited. Single-component excitation is approximated quite closely, however, at the $E_p = 953, 533$ and 811 keV resonances, where the decay of the $E_x = 2069, 2070$ and 2072 keV components constitutes 96.4, 94.5 and 86.6% of the total triplet decay, respectively. The branchings of the three components can now be determined with an iteration procedure, in which the values found at the above mentioned resonances serve as a first-order approximation.

The $E_x = 2069$ keV $4^+; 0$ component is simplest. It can only decay to the $5^+; 0$ and $3^+; 0$ states at $E_x = 0$ and 417 keV, respectively, except for a possible E2 branch to the 1759 keV $2^+; 0$ level, for which an upper limit of 0.013% was found. The

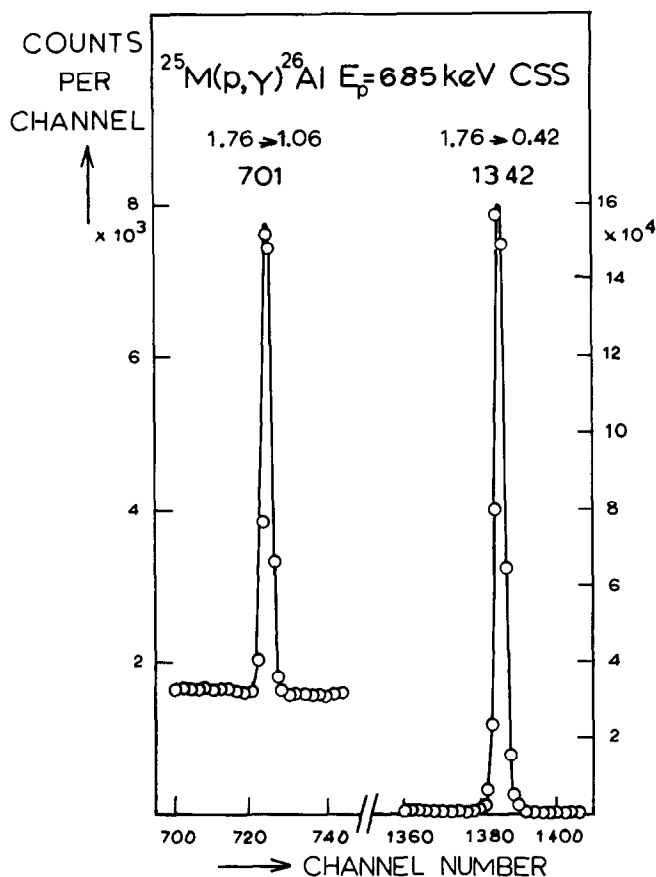


Fig. 3. The 2.0% $1.76 \rightarrow 1.06$ MeV decay branch as compared to the 98.0% $1.76 \rightarrow 0.42$ MeV main decay transition.

$2.07 \rightarrow 0$ MeV transition cannot occur in the decay of the other two components. Its intensity and the 2069 keV branchings given in table 6 can then be used to correct the $2.07 \rightarrow 0.42$ MeV intensity for a possible $2069 \rightarrow 417$ keV contribution at any resonance other than $E_p = 953$ keV.

We now turn to the 2070 keV $2^+; 1$ component which can decay to the 228 $0^+; 1$, 417 $3^+; 0$, 1058 $1^+; 0$, 1759 $2^+; 0$ and 1851 keV $1^+; 0$ states. The 2070 keV branchings have been obtained at the $E_p = 533$ keV $4^+; 1$ resonance, which is particularly suitable because the (secondary) feeding of the 2072 keV component (through the decay of the 2661 and 4548 keV levels) is extremely weak, only 0.04% of the feeding of the 2070 keV level. The previously unobserved very weak $2070 \rightarrow 1759$ keV branch has been seen at six resonances; statistics are best at $E_p = 723$ keV (fig. 4). Both the constant ratio of its intensity to that of the $2070 \rightarrow 1058$ MeV transition, and its energy determined at 90° , prove that it originates from the 2070 keV

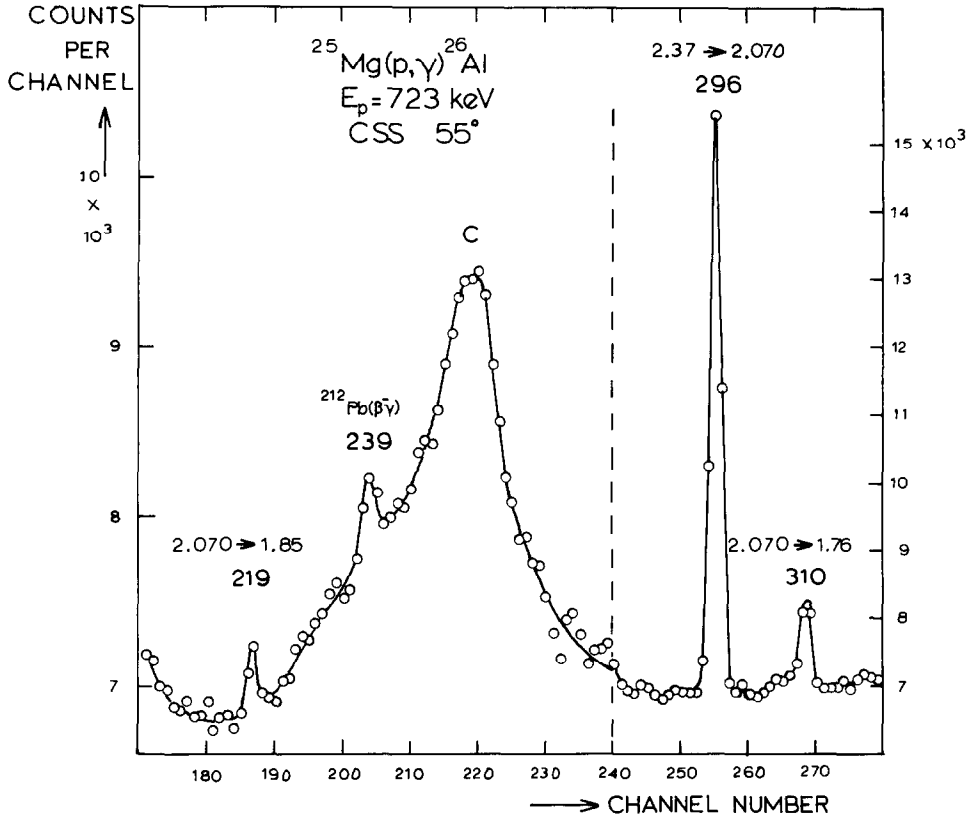


Fig. 4. The previously unobserved 2.070 → 1.76 and 2.070 → 1.85 MeV branches with branchings of 0.17 and 0.040%, respectively; C indicates the Compton ridge of the 0.42 → 0 MeV transition.

decay. The still weaker 2070 → 1851 keV branch (fig. 4) has been seen at three resonances.

We are now left with the 2072 keV $1^+; 0$ component, which previously was thought to decay 100% to the 228 keV level. This is certainly the strongest branch, but clearly a 2072 → 417 keV branch also exists, because at $E_p = 811$ keV with $J^\pi; T = 1^-; 1$ the 2.07 → 0.42 MeV is stronger than the 2.07 → 1.06 MeV line, whereas from the 2070 keV decay alone one would expect an intensity ratio of 21:75 (see table 6). Also the possibility of a relatively strong 2072 → 1058 keV branch should be considered. As said above, there is no resonance where the 2072 keV decay can be studied without interference from the omnipresent 2070 keV decay. Evidently, a single resonance is not enough to determine the total decay intensities of the 2070 and 2072 keV levels and the two branching ratios of the 2072 keV level (together four unknowns) from the intensities of the 2.07 → 0.23, 2.07 → 0.42 and 2.07 → 1.06 MeV lines (three input data). This difficulty can be overcome by a combined analysis of the decay at $E_p = 811$ and 1043 keV, the two resonances where the 2072 keV decay is relatively

strongest. The result is a 10.6(9)% $2072 \rightarrow 417$ keV branch and an upper limit of 3.0% for $2072 \rightarrow 1058$ keV. The extremely weak 0.043(8)% $2072 \rightarrow 1851$ keV branching and an upper limit of 0.05% for $2072 \rightarrow 1759$ keV have been obtained at $E_p = 811$ keV.

The absence of the $2072 \rightarrow 1058$ keV transition simplifies the decay analysis at other resonances. The $2.07 \rightarrow 0$ and $2.07 \rightarrow 1.06$ MeV intensities determine the 2069 and 2070 keV decay intensities, respectively, and the main decay branch of the 2072 keV level is then found by subtracting the 3.0% $2070 \rightarrow 228$ keV contribution from the $2.07 \rightarrow 0.23$ MeV intensity. The procedure can be checked by comparing the calculated intensity sum of the three $2.07 \rightarrow 0.42$ MeV contributions with its measured intensity, and by comparing the decay intensities (I_{out}) of the three components with the intensity sums of primary and secondary feeding transitions (I_{in}). The degree of agreement obtained is illustrated in table 7 for the $E_p = 928$ and 1084 keV resonances.

2.37 MeV. Excellent statistics for the decay of this level ($I_{\text{out}} = 2000\text{--}5000$) were obtained at five resonances. The branching ratios obtained (with a new branch to $E_x = 1.76$ MeV; see fig. 6) agree very nicely.

2.55 MeV. In many spectra the strong $E_\gamma = 476$ keV $2545 \rightarrow 2070$ keV decay line is disfigured by the 478 keV contaminant line from the $^7\text{Be}(\text{EC})^7\text{Li}$ decay with the ^7Be produced in the $^{10}\text{B}(p, \alpha)^7\text{Be}$ reaction. The intensity of this branch can thus only

TABLE 7
Intensity balance for the components of the $E_x = 2.07$ MeV triplet
at two $^{25}\text{Mg}(p, \gamma)^{26}\text{Al}$ resonances ^a

Decay from:	$E_p = 928$ keV, $1^+; 0$				$E_p = 1084$ keV, $4^-; 1$			
	2.069	2.070	2.072	total	2.069	2.070	2.072	total
I(2.07 \rightarrow 0)	<0.8				93			
I(2.07 \rightarrow 0.23)		[35.5]	[17.7]	53.2		[45.8]	[0]	45.6
I(2.07 \rightarrow 0.42)		[253]	[2.1]	[255] ^b	[206]	[326]	[0]	[532] ^c
I(2.07 \rightarrow 1.06)		892				1150		
I_{out}		1183	19.8		299	1525	0	
$I_{\text{prim.}}$		14			38			
$I_{\text{second.}}$		1221	24		258	1480	2.6	
I_{in}		1235	24		296	1480	2.6	

^a All E_x are in MeV. Calculated intensities are in square brackets.

For the definition of intensity, see table 2.

^b Measured intensity 266.

^c Measured intensity 495.

be derived as the difference between I_{in} and the intensity sum of the other decay branches. The weak ground-state decay is new.

2.66 MeV. The previously unobserved decay lines to the 1.76 and 1.85 MeV levels have been seen at many resonances. The 591 keV $2.66 \rightarrow 2.07$ MeV branch coincides within 0.4 keV with the previously unobserved $3.751 \rightarrow 3.16$ MeV transition. At most resonances the $2.66 \rightarrow 2.07$ MeV component predominates, but at $E_p = 986$ keV the $3.751 \rightarrow 3.16$ MeV component is stronger by a factor 4.5. The $2.66 \rightarrow 2.07$ MeV transition is also remarkable because not only the 2070 keV $2^+; 1$ but also the 2072 keV $1^+; 0$ level is excited. At the $E_p = 685$ and 1137 keV resonances the energy at 90° (as corrected for very small $3.741 \rightarrow 3.16$ MeV contributions) is measured as 591.28 (4) and 591.24 (4) keV, respectively. The average, 591.26 (3) keV, deviates markedly from the value 591.45 (6) keV expected for the $2.66 \rightarrow 2.07$ MeV decay. From the measured energy and the total $2.66 \rightarrow 2.07$ MeV branching one derives branchings of 24.6 (8) % and 3.4 (8) % for the transitions to the 2070 and 2072 keV levels, respectively.

2.74 MeV. The weak $2.74 \rightarrow 0.42$ MeV transition is new.

2.91 MeV. The branchings obtained at $E_p = 567, 986$ and 1043 keV are in excellent agreement. Just as for the $E_x = 2.55$ MeV level, the $E_\gamma = 844$ keV $2.91 \rightarrow 2.070$ MeV transition has to be regarded as a closing item in the branching sum, because at

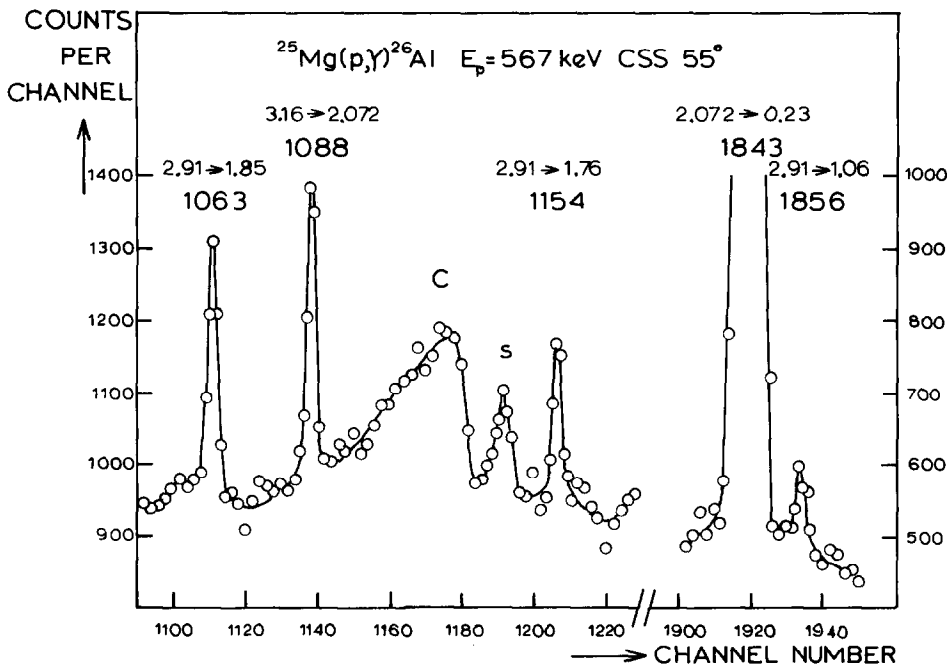


Fig. 5. Three previously unobserved branches in the decay of the $E_x = 2.91$ MeV level; C and s denote a Compton ridge and a single-escape peak of higher-energy lines, respectively.

several resonances it is contaminated with the $E_\gamma = 844$ keV line from the $^{26}\text{Mg}(p, \gamma)^{27}\text{Al}$ reaction. Three new weak branches are shown in fig. 5.

3.07 MeV. This level is best excited at the $E_p = 1103$ keV resonance, largely by secondary transitions. The decay at this resonance shows new branches to the $E_x = 1.76$ and 1.85 MeV levels, whereas possible branches to $E_x = 0$ and 0.42 MeV are obscured by other (stronger) transitions. The latter two branches show up clearly at $E_p = 969$ and 1649 keV.

3.16 MeV. The decay of this level has been discussed already in ref. ¹²). The four weak branches not yet listed in ref. ¹¹) are shown in fig. 6, as observed at $E_p = 881$ keV. The statement in ref. ¹³) that the decay feeds the $E_x = 2070$ and not the 2072 keV level is definitely erroneous, as proven both by the $3.16 \rightarrow 2.07$ MeV γ -ray energy and by the intensity balance at the final state, at several resonances. The relative

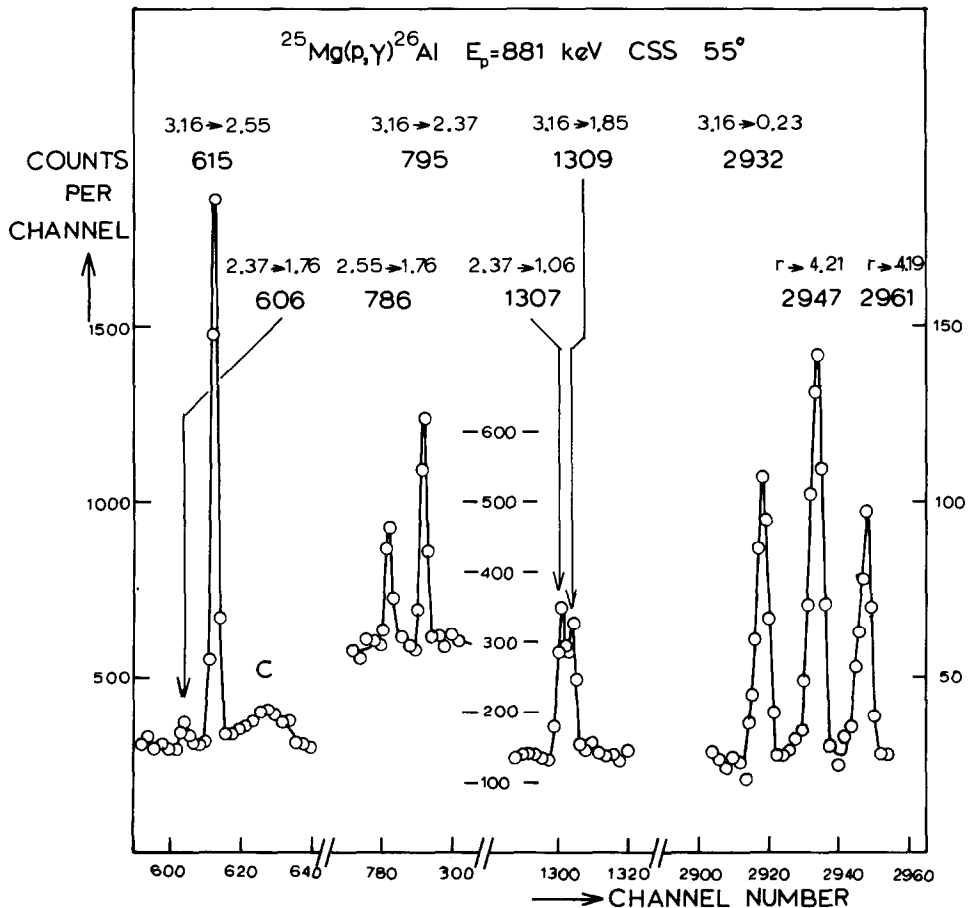


Fig. 6. Four previously unobserved branches in the decay of the $E_x = 3.16$ MeV level; the new $2.37 \rightarrow 1.76$ MeV branch is also shown.

TABLE 8

Branching ratios for the decay of the 3.16 MeV 2^+ ;1 level as determined at six resonances ^a

E_p [keV]	$J^\pi_f; T_f$	I_{in}	Decay to:	0.23	0.42	1.06	1.76	1.85	2.069	2.070	2.072	2.37	2.55	2.66
			$J^\pi_f; T_f$:	$0^+; 1$	$3^+; 0$	$1^+; 0$	$2^+; 0$	$1^+; 0$	$4^+; 0$	$2^+; 1$	$1^+; 0$	$3^+; 0$	$3^+; 0$	$2^+; 0$
775	$3^+; 0$	1407		0.44	[100]	25.9	21.6				3.94		2.14	
881	$3^+; 0$	1902		0.63	[100]	25.4	21.8	0.58			3.97	0.54	1.92	<0.05
969	$3^-; 0$	1313			[100]		23.0				4.43	0.34	2.21	
986	$2^-; 1(+0)$	1169		0.71	[100]	25.7	23.2				4.02		2.28	
1196	$1^+; 0$	1781		0.64	[100]	26.8	23.9	0.53			4.43	0.29	2.26	
1302	$2^+; 0$	4845		0.81	[100]	25.5	23.6				4.39	0.30	2.39	<0.06
$\langle \text{Relative intensity} \rangle_{av}$:				0.69	[100]	25.8	23.0	0.56			4.25	0.34	2.25	<0.05
Branching ratio [%] :				0.44 ₅	63.7 ₇	16.4 ₅	14.7 ₄	0.35 ₃	<0.014 ^b	<0.4 ^c	2.71 ₈	0.22 ₅	1.43 ₅	<0.03

^a Relative intensities are given (normalized on the intensity of the strongest branch) which, in the last line, are converted into branching ratios.

^b As determined from the lifetime (table 11) and the RUL for E_{21S} .

^c As determined from $E_\gamma(3.16 \rightarrow 2.072 \text{ MeV})$.

decay intensities obtained at six resonances are compared in table 8. The resulting average branching ratios supersede those given in ref. ¹²⁾ in which only the data at $E_p = 775$ and 881 keV had been used. The differences between the values given in ref. ¹²⁾ and in the present work are quite small. The $3.16 \rightarrow 1.85$ MeV branch is only clearly seen at $E_p = 881$ keV (fig. 6) and at $E_p = 1196$ keV, which are the only resonances where the ever-present $E_\gamma = 1307$ keV $2.37 \rightarrow 1.06$ MeV transition does not completely swamp the $E_\gamma = 1309$ keV $3.16 \rightarrow 1.85$ MeV transition.

The 3.68 MeV doublet. The decay of the $E_x = 3675$ and 3681 keV levels is best observed at $E_p = 1205$ and 685 keV, respectively, with corroborating evidence obtained at $E_p = 953$ and 1237 keV for the former, and at $E_p = 1205$ and 1237 keV for the latter level.

The 3.75 MeV doublet. There are several resonances where the decay of the 3751 keV component can be studied without interference from the 3754 keV decay, and vice versa. The difficulty of the coinciding $3.751 \rightarrow 3.16$ and $2.66 \rightarrow 2.07$ MeV transitions has been mentioned above. The branching for the $E_\gamma = 1014$ keV $3.754 \rightarrow 2.74$ MeV transition coinciding with the strong 1012 keV $2.070 \rightarrow 1.06$ MeV line has been derived by means of the intensity balance at the 2.74 MeV level.

3.98 MeV. Until recently, the evidence for the existence of this level could not be considered as very strong. It had only been observed with the $^{24}\text{Mg}(\tau, p\gamma)^{26}\text{Al}$ reaction ¹⁴⁾ (decay to the 1.06 and 1.85 MeV levels; no branchings reported) and, very weakly, with the $^{27}\text{Al}(p, d)^{26}\text{Al}$ reaction ¹⁵⁾. It did not seem to be excited at any of the lower-energy (p, γ) resonances until, finally, we found it to be fed quite

strongly at the $E_p = 1763$ and 1800 keV resonances, with branchings of $b = 22.8$ (7) % and 6.3 (9) %, respectively. With the excitation energy well determined, it was then seen to be weakly excited also at $E_p = 516, 656, 811$ and 1184 keV (see table 5), and in the decay of the bound states at $E_x = 6028$ and 6238 keV. The reluctance of so many higher states to decay to this relatively low-energy level may be explained by its unusual J^π value, $J^\pi = 0^-$, as determined recently with the $^{28}\text{Si}(\vec{d}, \alpha)^{26}\text{Al}$ reaction¹⁶⁾.

4.48 MeV. This level is also excited at only six resonances (table 5), presumably for the same reason as for the $E_x = 3.98$ MeV level: it also has $J^\pi = 0^-$ [refs. ^{16,25)}].

4.55 MeV. The seven previously unobserved branches are shown in fig. 7.

The 4.94 MeV. doublet. The level previously known¹¹⁾ at $E_x = 4938.1$ (9) keV has been resolved into a doublet with components at 4939.64 (9) and 4940.79 (5) keV. The lower component is strongly excited at the $E_p = 811, 1763$ and 1800 keV resonances, with $b = 3.6$ (1) %, 13.2 (4) % and 5.1 (7) %, respectively, and weakly at 16 other resonances. The upper component is excited with $b = 3.6$ (2) % at the weak $E_p = 609$ keV resonance and still more weakly at 11 other resonances. The decay modes of the two levels are quite different, without a single branch in common.

The 5.01 MeV doublet. The level previously known at $E_x = 5006$ (3) keV from the (p, d) reaction¹⁵⁾ also turned out to be a doublet, with components at $E_x =$

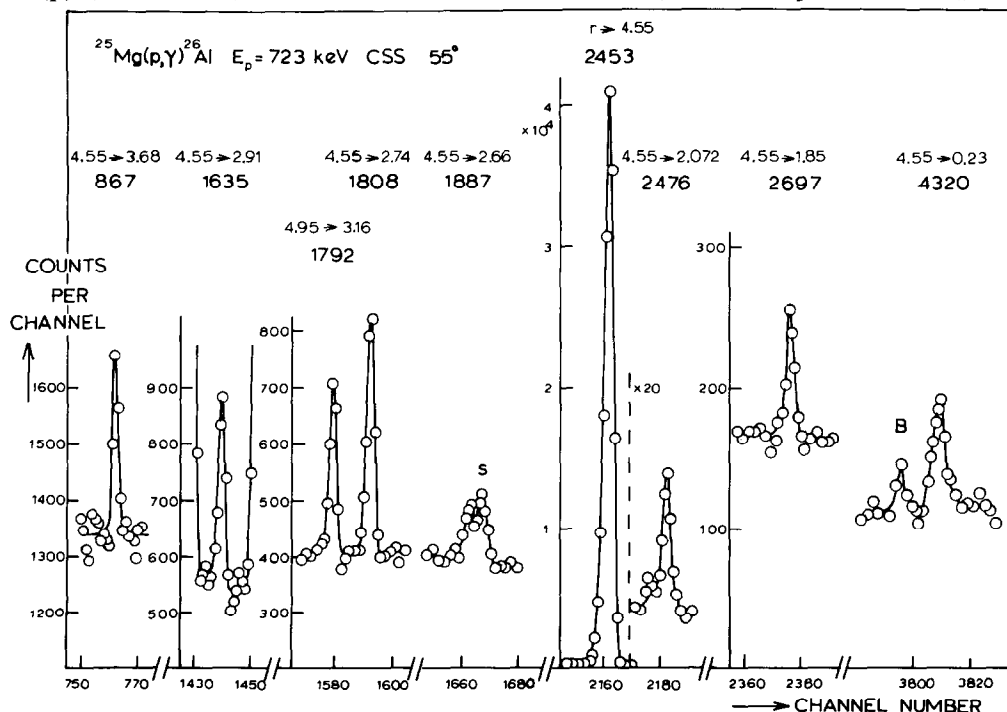


Fig. 7. Seven previously unobserved weak ($b = 0.2$ – 1.2%) branches in the decay of the $E_x = 4.55$ MeV level; B and s denote background and single-escape peaks, respectively. The $r \rightarrow 4.55$ MeV primary is also shown.

5006.66 (16) and 5010.24 (7) keV, again with very different decay, without a single branch in common. The levels are weakly excited at 19 and 14 resonances, respectively.

5.20 MeV. The energy of this level had been determined as 5.194 (5) keV from the (p, d) reaction ¹⁵, and as 5194 (4) keV from the $^{25}\text{Mg}(p, \gamma)^{26}\text{Al}$ reaction at the $E_p = 1196$ keV resonance ¹³. It turns out to be also weakly excited at 12 other resonances, with the energy now determined as $E_x = 5195.11$ (12) keV.

The 5.46 MeV doublet. The well-known lower-energy component at $E_x = 5456.71$ (5) keV, could be studied very well. It is excited at 30 resonances, at some quite strongly, and 15 decay branches have been observed.

The (new) upper component, at $E_x = 5461.87$ (13) keV, proved to be much more evasive, with weak excitation at only three resonances (see table 5).

The 5.49 MeV doublet. The level previously observed with the (p, d) reaction ¹⁵ at $E_x = 5491$ (3) keV (nothing known about the γ -decay), has been resolved into a doublet with components at $E_x = 5487.93$ (6) and 5494.51 (5) keV which are weakly excited at 7 and 27 resonances, respectively, and of which the decay is entirely different.

The 5.67 MeV doublet. The lower component, at $E_x = 5671.04$ (7) keV, weakly excited at 17 resonances, has not been previously observed. The well-known upper component, at $E_x = 5676.07$ (5) keV, is excited at still more resonances, at some quite strongly, and thus its decay could be studied very well.

The 5.92 MeV doublet. The two components, at $E_x = 5916.10$ (6) and 5924.19 (7) keV, are both excited at many resonances, with the upper component previously unobserved.

The 6.08 MeV doublet. Of the two levels at $E_x = 6084.07$ (5) and 6086.47 (11) keV the upper one had not been observed earlier.

6.50, 6.55 and 6.60 MeV. The levels at $E_x = 6496$, 6551 and 6598 keV have been seen ¹⁰) as extremely weak (p, γ) resonances at $E_p = 197$, 255 and 304 keV, respectively. For the (p, γ) feeding of these levels, see table 5. For the 6496 keV level our branchings are superior to (and compatible with) those given in ref. ¹⁰), for $E_x = 6551$ keV we present the averages of the two sets of branchings, whereas for the 6598 keV level the branchings of ref. ¹⁰) are much better than ours.

In the discussion given above seven levels, all components of close-lying doublets, have been mentioned which had not been previously observed at all. The levels at $E_x = 5431$, 5495, 5569, 5598, 5883 and 5950 keV, and the remaining nine levels in the $E_x = 6.10$ –6.45 MeV region, had been seen in previous particle transfer work ^{8,11}), but not in (p, γ). All levels observed from particle transfer are also excited in (p, γ), with the possible exception of a level at $E_x = 6005$ (10) keV which is claimed to have been observed by Betts *et al.* ⁸) with the (τ , d) reaction; no corresponding peak is visible in their $\theta = 19^\circ$ deuteron spectrum (their fig. 1). The levels above $E_x = 6.6$ MeV have been discussed in ref. ¹).

Just as for the resonance branchings, the agreement between the secondary state branchings given in ref. ²⁾ with those in table 6 is excellent, if the much lower statistical quality of the former data is taken into account. Of the 119 unbracketed branchings listed in ref. ²⁾, there is only one, the $E_\gamma = 750 \text{ keV } 4.43 \rightarrow 3.68 \text{ MeV}$ transition, for which their $b = 8 (3) \%$ compares badly with our upper limit of 1%.

TABLE 9
Decay of levels observed in resonance \rightarrow resonance
transitions

E_p	E_x	E_p^a	I_{in}^a	Γ_γ/Γ		
[keV]	[keV]	[keV]		I_{out}/I_{in}^b	GRSS ^c	$(p, p_0)^d$
<6610				≈ 1		
317	6610	1306	4.2		≈ 0	
390	6680	1306	104	0.184		
435	6724	1137	13.1		≈ 0	
497	6784	1184	0.7		≈ 0	
503	6789	1829	7.9		≈ 0	
515	6801	1306	4.1		0.7512	
516	6802	1302	15.6		0.5811	
	6816	1375	59	≈ 1		
533	6818	1205	22.2	≈ 1	0.96017	
567	6852	1525	5.9		≈ 0	
591	6874	1829	7.1		0.885	
593	6876	1525	3.9		≈ 0	
609	6892	1833	83	0.03217		$\approx 0^e$
685	6964	1580	3.0			$\approx 0^e$
723	7001	1699	3.4		≈ 0	
738	7015	1714	12.4	<0.5	0.749	
835	7109	1714	49.6	<0.25		≈ 0
953	7222	1680	4.4		≈ 0	
1025	7291	1714	30.2	<0.7		≈ 0
1084	7348	1680	2.7			≈ 0

^a Resonance with best feeding. ^b As obtained at best feeding resonance. ^c From γ -ray strength statistics ³⁾.

^d From the $^{25}\text{Mg}(p, p_0)$ reaction ²⁶⁾, if not mentioned differently.

^e Because of strong excitation in the $^{25}\text{Mg}(\alpha, t)^{26}\text{Al}$ reaction ²⁷⁾ Γ_p should be relatively large, and thus $\Gamma_\gamma/\Gamma \approx 0$.

At the $E_p = 835$ keV resonance where the excitation of the 4.43 MeV level is strongest, a line is observed at $E_\gamma = 745$ keV but it has to be interpreted as the $r \rightarrow 6.36$ MeV primary.

For the decay of the $E_x = 4480$ and 5916 keV levels, see also ref. ²³).

Finally we should discuss the γ -decay of levels above the proton binding energy, as observed when they are excited from higher-lying resonances, because a comparison of I_{in} and I_{out} provides the ratio Γ_γ/Γ . The ratios thus obtained are listed in table 9 column 5, as compared to the Γ_γ/Γ values found from γ -ray strength statistics (GRSS) and from the $^{25}\text{Mg}(p, p_0)$ reaction ²⁶). All levels below $E_x = 6610$ keV, in addition to the $E_x = 6816$ and 6818 keV levels, have $I_{\text{out}}/I_{\text{in}} = \Gamma_\gamma/\Gamma \approx 1$. The 6816 keV level (already mentioned in sect. 3) probably has $J^\pi = 6^+$ and thus $I_p = 4$ with a correspondingly small Γ_p . The $\Gamma_\gamma/\Gamma \approx 1$ value for $E_x = 6818$ keV agrees with that obtained from GRSS. For the $E_x = 6680$ and 6892 keV levels definite Γ_γ/Γ values are given, which together with the (p, γ) resonance yields determine Γ_p and Γ_γ . For another three levels with relatively large I_{in} upper limits of Γ_γ/Γ could be deduced. For the remaining levels I_{in} is too small, or the decay is too much split up into weak branches, to say anything meaningful.

5. Energies

Most energies have been determined from the 90° spectra taken with an unshielded detector. They have the advantage that transitions are not Doppler shifted, but the disadvantage of greater complexity because of the many escape peaks. Of the about 100–120 transitions observed at a resonance, about 50% might be situated in the $E_\gamma = 1.5$ –4.0 MeV region. With the escape peaks taken into account the peak density in this region is seen to be large, and correspondingly there will be many composite peaks which are unsuitable for accurate energy determinations.

In the 55° CSS spectra the probability of a peak being uncontaminated is much larger. These spectra can be energy calibrated, first by using primaries which generally can be considered as being fully Doppler shifted, second by using decay transitions from very long-lived states ¹¹) ($E_x = 0.42, 1.76, 2.37, 2.55$ and 2.66 MeV) which can be considered unshifted, and third by using the decay lines of the very short-lived 3.16 MeV level (strongly excited at many resonances) of which the lifetime has been determined quite accurately ¹²). The $E_\gamma = 585$ and 975 keV lines from $^{25}\text{Mg}(p, p')$ are also suitable for calibration purposes; they deexcite long-lived ^{25}Mg levels.

The energy calibration was performed in two steps. As a basis served the accurate excitation energies ($\Delta E_x = 3$ –70 eV) of ten levels below 3.0 MeV with, in addition, those at 3.16 and 3.72 MeV, all reported in ref. ¹⁷) (see table 10). Later the energies of the 2.070 and 2.072 MeV levels were added to this group ¹²). The decay lines of these levels cover the low-energy part of the spectra ($E_\gamma = 0.29$ –2.75 MeV); the $E_\gamma = 3495$ keV $3.72 \rightarrow 0.23$ MeV transition is seen at only a few low-spin resonances. To cover the need for higher-energy calibration lines, spectra were taken, as a second

step, at the $E_p = 986$ and 1043 keV resonances simultaneously with a ^{66}Ga radioactive source. Of many ^{66}Ga lines the energies, stretching from 686 to 4806 keV, are known quite accurately¹⁹⁾. The measurements were performed, as in ref.¹⁷⁾, with the unshielded detector alternately at $+90^\circ$ and -90° (to average out errors in the 90° position), and with target and source irradiating the detector from the same direction. These measurements provided the excitation energies of ten levels in the $E_x = 3.5\text{--}5.7$ MeV region ($\Delta E_x = 50\text{--}140$ eV), in addition to that at $E_x = 3.72$ MeV.

Resonance and bound-state energies at the other resonances were finally obtained from the 90° spectra by internal calibration on the decay lines of the 22 levels mentioned above. Once the resonance energy is known (and thus the energies of many primaries) the 55° spectrum can also be used to obtain further information, as already explained. The procedure is to some extent a matter of chance. At many resonances three or more primaries with energies in the well-calibrated region could be used to obtain the resonance energy. At some resonances, however, only a single primary was usable, with the other primaries either being too weak, or contaminated, or outside the well-calibrated region. No escape peaks were used in energy determinations because it is well known¹⁷⁾ that their energies differ systematically from $E_\gamma - mc^2$ and $E_\gamma - 2mc^2$, respectively. The 511 keV annihilation line was not used either, nor any background lines.

The final errors assigned to transition energies (corrected for nuclear recoil) contain, in addition to the statistical error, two more components. The estimated calibration error depends on the quality of the calibration curve fitted through the calibration points and on the errors of the latter; it is generally much smaller in the low- than in the high-energy part of the spectrum, and strongly differs from spectrum to spectrum. A second component accounts for the accuracy (estimated as 1°) with which the 90° detector can be positioned. Such a deviation from 90° would introduce a Doppler shift which for infinitely fast transitions increases from 18 ppm at $E_p = 317$ keV to 43 ppm at 1833 keV. This “ 1° error” may be the dominant contribution to the final error for high-energy levels, in particular for the resonances. A rough check (accurate to about 2°) on the position of the 90° detector is provided by the requirement that calibration points resulting from the decay of both short-lived and long-lived levels lie on the same smooth calibration curve. For each resonance the two detectors were positioned anew, such that energies obtained at different resonances can be considered as statistically independent. The latter assumption is not quite correct because all determinations are based on the same set of calibration energies, of which the errors are not quite statistically independent either. The interdependence of errors is far too complicated to be taken into account exactly but, anyway, the effect was recognized and correspondingly final errors were rounded off upwards by an estimated amount if they seemed unrealistically small.

The secondary-state excitation energies obtained at different resonances are listed in table 10; the resonance energies have already been given in ref.¹⁾. Table 10 contains 225 entries determining the energies of 72 levels in the $E_x = 1.8\text{--}6.9$ MeV

TABLE 10

Excitation energies (in keV) of ^{26}Al secondary states as determined at different resonances (E_p in keV); last column gives $E_x(\text{average})^a$

390 1850.645	, 515 .628	, 593 .666	, 811 .536	, 1043 .627	, 1850.623
	1135 .702	, 1184 .627	, 1196 .617	, 1306 .628	
533 2068.936	, 685 .777	, 738 .877			2068.865
533 3073.5712	, 685 .7913	, 738 .607	, 1137 .636		3073.634
533 3402.7510	, 738 .5715	, 953 .5510	, 1026 .7516		3402.656
609 3507.8112	, 953 .3221	, 1103 .8918	, 1375 .6211	, 1774 .4715	3507.638
			1763 .8715		
317 3596.326	, 738 .276	, 1043 .405			3596.344
533 3675.0617	, 738 4.9910	, 890 5.0214	, 953 4.818		3674.925
835 3680.7712	, 1026 .5318	, 1137 .677			3680.686
567 3723.6914	, 723 .5917	, 811 .7811	, 1043 .828	, 1283 .9820	3723.795
			1525 .8217	, 1763 .8715	
775 3751.0814	, 986 0.846	, 1043 0.906			3750.904
811 3753.732	, 928 .4512				3753.6313
738					3921.9624
533 3962.807	, 738 .942	, 775 .8222	, 1205 .7710		3962.835
1763					3977.912
390 4191.9410	, 986 1.858	, 1137 2.0312			4191.926
738 4206.0312	, 953 5.8410	, 1205 5.927	, 1237 5.776		4205.865
723 4349.2211	, 738 .2317	, 1043 .462	, 1137 .3514		4349.347
835 4430.697	, 969 .8921	, 1084 .8018			4430.726
811					4480.482
390 4547.9310	, 723 .8510	, 1137 .9710			4547.926
390 4599.115	, 435 .166	, 881 .2910	, 1026 .3512		4599.175
811 4622.4317	, 890 .3211	, 986 .388	, 1283 .397		4622.385
435 4705.406	, 738 .298	, 835 .1812	, 969 .372	, 1103 .4714	4705.374
			1205 .4511	, 1237 .1716	
738 4773.3615	, 835 .3811	, 935 .322			4773.356
811 4939.6111	, 890 .6916	, 1283 .7126			4939.642
533 4940.818	, 1375 .792	, 1714 .768			4940.795
593 4952.288	, 723 .1915	, 1205 .346	, 1237 .285	, 1342 .302	4952.304
			1649 .1810	, 1699 .4911	
685 5006.6320	, 1137 .7026				5006.6616
811 5010.1012	, 1043 .267				5010.247
738 5131.752	, 775 2.028	, 896 1.886	, 1026 2.1110	, 1103 1.937	5131.935
390 5141.7711	, 567 .6312	, 723 .6310	, 738 .7318		5141.686
591 5195.0010	, 1196 .4520	, 1370 .2222			5195.1112
738 5245.347	, 953 .1710	, 1375 .276			5245.284
685 5395.512	, 1714 .6118	, 1833 .5516			5395.537
497 5431.3734	, 656 .2520	, 811 .3115	, 969 .0612		5431.2310
685 5456.708	, 969 .682	, 1137 .742			5456.715

TABLE 10 - continued

1763							5461.8713
533	5487.9820,	609	.947,	1714	.9111		5487.936
685	5494.5114,	1164	.5511,	1205	.5912,	1237	.486
953	5513.3115,	1237	.486,	1714	.516		5513.484
390	5544.592,	890	.5112				5544.567
533	5568.9623,	1680	9.3422				5569.1619
1043							5584.996
685	5598.3111,	835	.5422,	896	.278		5598.306
567	5670.9212,	656	1.1417,	811	1.0812,	1043	1.1014
503	5676.099,	685	.078,	1137	.0411		5676.075
870	5692.232,	896	.127,	986	.127		5692.155
738	5726.3510,	890	.2614,	969	.4210,	1103	.4814,
811	5849.2822,	1137	.0518,	1237	.1314,	1306	.3312
1744	5882.6512,	1829	.6512				5882.652
685	5916.088,	811	.1213,	870	.155		5916.106
515	5924.1217,	835	.1510,	890	.3314		5924.197
567	5950.086,	656	50.0218,	811	49.9716,	1135	49.7513
656	6027.958,	723	7.9515,	1135	8.045		6028.024
835	6084.029,	1084	.2217,	1148	.026,	1714	.1710
811	6086.4822,	1283	.4712				6086.4711
953	6119.992,	1375	20.0310				6120.017
1179	6197.5622,	1763	.5641				6197.5619
1763							6238.3826
533	6253.74,	969	4.27,	1205	4.34,	1829	3.94,
1306						1833	4.45
567	6280.4013,	593	.4017,	986	.0820		6280.339
953	6343.5411,	1375	.3811				6343.468
390	6363.8930,	835	3.8810,	890	4.1114,	1084	4.2120
1205							6398.6421
928	6414.2822,	1370	.5111				6414.4610
1714							6436.4411
953	6495.8717,	1680	6.1325,	1714	5.948		6495.947
1084	6550.5121,	1148	.707				6550.687
1714							6598.3216
1196	6801.7021,	1302	.4526				6801.6016
1375	6815.7013,	1774	.9929,	1833	.7322		6815.7410

^a Second and following entries have been shortened by omitting those decimals in E_x which are the same for all entries; for example (first line), for 515 .628 read 515 1850.628.

TABLE 11

Comparison of present ^{26}Al secondary-state excitation energies (in keV)
with those from previous work ^a

Present			Previous work		
work					
	ref. 11)	other	work	ref. 11)	other
	228.4415	228.30513 ^b	5141.686	5140.816	
	416.83	416.8523 ^b	5195.1112	51945	51944 ^e
	1057.75	1057.73912 ^b	5245.284	5244.116	
	1759.05	1759.0348 ^b	5395.537	5393.79	5393.412 ^d
1850.623	1850.36	1850.62070 ^b	5431.2310	542810	
2068.865	2068.73		5456.715	5454.918	5455.76 ^d
	2069.53	2069.473 ^c	5461.8713		
	2071.57	2071.644 ^c	5487.936		
	2365.04	2365.15018 ^b	5494.515	54913	
	2545.25	2545.36717 ^b	5513.484	55132	
	2660.84	2660.92050 ^b	5544.567	55422	
	2739.27	2740.03030 ^b	5569.1619	55663	
	2913.05	2913.40050 ^b	5584.996	5583.015	
3073.634	3073.010		5598.306	55953	
	3159.67	3159.88913 ^b	5671.047		
3402.656	3403.34		5676.075	5673.92	
3507.638	3507.55		5692.155	5691.014	
3596.344	3595.712		5726.385	5724.719	
3674.925	3673.512		5849.218	5847.119	
3680.686	3680.812		5882.659	58796	
3723.795	3723.212	3723.86070 ^b	5916.106	5913.510	
3750.904	3749.818		5924.197		
3753.6313	3753.110		5949.938	59466	
3921.9624	3922.519		6028.024	60245	
3962.835	3962.710		6084.075	60832	6083.48 ^d
3977.919	39791		6086.4711		
4191.926	4191.314		6120.017	61236	
4205.865	4205.214		6197.5619	61996	
4349.347	4348.816		6238.3826		
4430.726	4429.911		6254.0620	62476	
4480.489	4479.410		6270.1911	62715	
4547.926	4547.216		6280.339		
4599.175	4598.513		6343.468	63465	6345.67 ^d
4622.385	4622.015		6363.998	636210	6363.311 ^d
4705.374	4705.111		6398.6421	63995	6397.518 ^d
4773.356	4771.616	4772.412 ^d	6414.4610		6410.312 ^d
4939.649	4938.19	4938.817 ^d	6436.4411	64355	6435.55 ^d
4940.795			6495.947	64985	6494.813 ^{f,g}

TABLE 11 - continued

Present work	Previous work		Present work	Previous work	
	ref. 11)	other		ref. 11)	other
4952.304	4951.712		6550.687	65556	6549.314 ^f
5006.6616			6598.3216		6597.912 ^f
5010.247	50063		6801.6016		
5131.935	5131.42		6815.7410		

^a For $^{25}\text{Mg} + p$ resonances in the $E_x = 6.6 - 8.1$ MeV region, see ref. 1).

^b Ref. 17). ^c Ref. 12). ^d Ref. 18). ^e Ref. 13). ^f Ref. 10).

^g Also 6498.312 keV in ref. 18).

region with errors between 30 and 260 eV. Many of the entries are averages of the E_x values obtained from different decay branches and/or the primary. For the 62 levels for which E_x was determined at more than one resonance we find $\chi^2/(N-62) = 0.79(12)$, where N is the total number of entries (215) for these levels. The small χ^2 value gives us the reassuring feeling that few (if any) of the lines used were seriously contaminated, that the 1° estimate for the error in the 90° detector position was not unduly small and, finally, that the energies of the large set of internal calibration lines used did not show any gross discrepancies.

In table 11 the present secondary-state excitation energies are compared with those from previous work^{7,10-13,18}). The present errors (average 0.10 keV) are about an order of magnitude smaller than those from previous (p, γ) work (1-2 keV), and up to two orders of magnitude smaller than those from previous particle work (3-10 keV). Apparently previous (p, γ) energies²⁾ are very slightly low (see fig. 8), with the difference increasing from ~ 0.6 keV for $E_x = 3-4$ MeV to ~ 1.2 keV for $E_x = 5-6$ MeV, but only for a single level ($E_x = 5916$ keV) the difference exceeds twice the error.

6. Lifetimes

A proper (p, γ) DSA lifetime determination requires a measurement of γ -ray spectra (with the same detector) taken alternately at $\theta = 0^\circ$ and at an angle as far backwards as possible (in practice $\theta \sim 120^\circ$). A thick target should be used and the proton energy should be chosen only slightly above the resonance energy, so as to ensure that the capture reaction takes place in the front layer of the target and that recoils stop in the target material and not in the backing.

Such (time consuming) measurements have not been performed. The present 55° spectra, however, with their accurate energy calibration also contain Doppler shift information, although the decay line shifts (relative to $\theta = 90^\circ$) are only 38% of those for the full 0- 120° range.

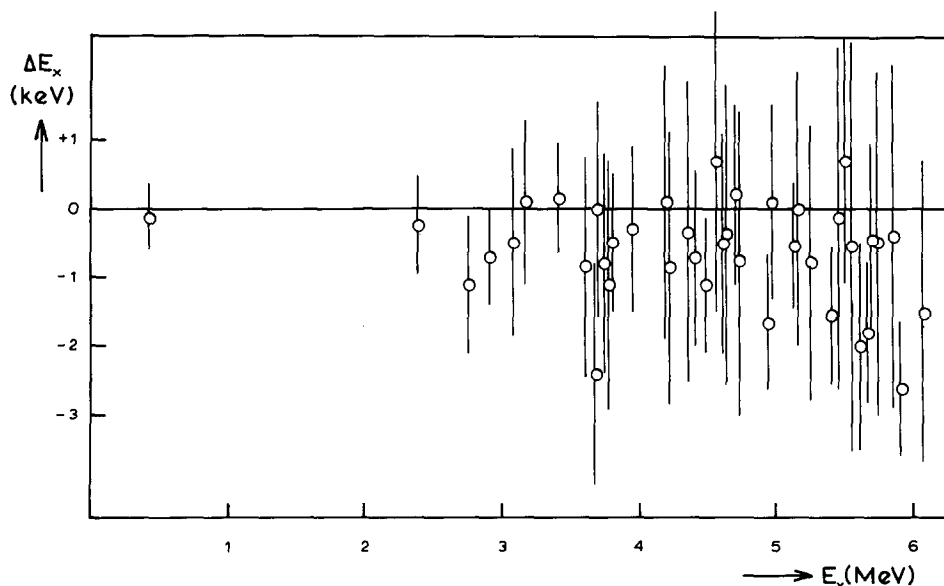


Fig. 8. Differences of the excitation energies of ^{26}Al levels given in ref. ²⁾ and in the present work, E_1 and E_2 , respectively; $\Delta E_x = E_1 - E_2$. Errors are those of ref. ²⁾; the present errors are smaller by more than an order of magnitude.

The use of the available 55° spectra for the extraction of lifetimes, with the latter regarded as a byproduct relative to branchings and excitation energies, has two drawbacks in addition to the small shifts. First many of the targets used could not be regarded as thick especially at the higher-energy proton resonances, such that part of the recoil stopping took place in the backing. This point was taken into account in the programme based on the Blaugrund formalism ²⁰⁾ which calculates the attenuation curve $F(\tau_m)$ for converting observed shifts into mean lives. The predominant nuclear component in the stopping power was taken from ref. ²¹⁾. Because target thicknesses, determined by weighing, were none too well known, the $F(\tau_m)$ curves cannot be considered as very accurate. The second difficulty is that the peak fitting programme used (sect. 2) determines the energy at the top of the peak, rather than the centroid energy which should be used for the lifetime calculation. The result is that for decay lines from relatively short-lived levels (with a tail on the low-energy side induced by the Doppler effect) the peak energy (and thus the energy shift) comes out too high, whereas for long-lived levels it is the opposite. This effect, steepening the $F(\tau_m)$ curve, has not properly been taken into account.

Along the lines sketched above, lifetimes (or lifetime limits) have been determined from the 55° spectra for 63 ^{26}Al levels. For many levels results were obtained at several (up to ten) resonances, and for many levels several (up to eight) decay lines

could be used. Cases where indirect feeding contributed more than 15% were not taken along.

In the analysis, targets were considered as being oxidized (MgO). In a separate α -particle Rutherford back-scattering experiment, a target evaporated onto a carbon disc proved to be completely oxidized.

For 44 levels previous lifetime information from 0-120° DSA measurements^{11-13,23)} is available (see table 12), which is considered superior to our own, because of the reasons given above. Generally the agreement of our results with the adopted values in table 12 is reasonable although on the average our short lifetimes are somewhat shorter and the long lifetimes somewhat longer than those given in table 12 (as expected). The lifetimes obtained for another 32 levels for which no

TABLE 12
Lifetimes of ^{26}Al levels from previous work

E_x [keV]	τ_m [fs]			E_x [keV]	τ_m [fs]		
	ref. 11)	refs. 13,23)	adopted		ref. 11)	ref. 23)	adopted
417	1.805x10 ⁶		1.805x10 ⁶	3922	286		286
1058	367		367	3963	5410	5411	547
1759	6000500		6000500	4192		73	73
1851	4010	475	465	4206		9015	9015
2069	45070		45070	4349	<15	134	134
2070	174	223	203	4480	11030	8020	9017
2072	48050	730100	530100	4548	<15		<15
2365	1400300		1400300	4599		73	73
2545	1000250		1000250	4622		7626	7626
2661	3000400		3000400	4705	<15	<5	<5
2740	468	417	435	4773		11817	11817
2913	8812	1017	986	4940	11030	9327	10020
3074	21060	31040	28045	4952		144	144
3160	3610	92, 83	62 ^a	5132	<15	<5	<5
3403	7419	11015	9618	5142		<6	<6
3508	236	268	245	5245		174	174
3596	3610	244	264	5396		9570	9570
3675	26070	22030	22530	5513		516	516
3681	2712	122	122	5545		2219	2219
3724	<23	62	62	5585		<8	<8
3751	309	3716	328	5676		3214	3214
3754	292	73	73	5916		<3	<3

^a Included is $\tau_m = 4.912$ fs from ref. 12).

TABLE 13

The DSA attenuation factors and corresponding mean lives of some ^{26}Al levels (not listed in table 11) as measured at different resonances in the present work ^a

E_x [keV]	E_p [keV]	$F(\tau_m)$	$\langle F(\tau_m) \rangle_{av}$	τ_m [fs]
3978	1763		0.023	>1500
4431	835	0.524 , 1137 0.585 , 1763 0.634	0.583	8512
4941	1375	0.85621, 1714 0.903	0.87017	358
5007	658	0.312 , 896 0.418 , 1763 0.384	0.37535	17545
5010	1043	0.97525, 1135 0.98522, 1744 1.015	0.98312	<9
5195	591	1.055 , 1196 0.8110	1.0110	<35
5431	811		0.894	178
5457	685	0.817 , 1084 0.806 , 1137 0.884 ,	0.85223	246
	1148	0.865 , 1283 0.915		
5462	1763		0.947	<30
5488	1714		0.854	258
5495	685	0.976 , 1306 0.963 , 1744 1.033	1.00012	<7
5598	896		0.845	2710
5671	811	0.882 , 1283 0.9512	0.927	<40
5692	835	0.946 , 896 0.964 , 969 1.005 ,	0.9752	4.016
	986	0.97013, 1084 1.023 , 1148 0.97014		
5726	738	0.98513, 969 1.007	0.98513	<7
5849	1205	0.907 , 1699 0.946	0.925	148
5883	1744	1.01030, 1829 0.93522	0.974	<17
5924	969		1.035	<17
5950	811		0.922	<40
6028	1135		1.00116	<6
6084	896	0.4414 , 1084 0.454 , 1148 0.464	0.45722	13030
6086	811		0.882	2016
6120	953	0.8911 , 1375 0.91412	0.91412	155
6238	1763		1.013	<10
6270	1306		1.034	<13
6280	1699		0.956	<20
6343	953	1.078 , 1375 1.013 , 1699 0.985	1.00924	<8
6364	896		0.828	3216
6436	1714		1.027	<24
6496	1714		0.993	<12
6816	1375		0.996	<22

^a All measured F-values have been converted to those for an infinitely thick MgO target at $E_p = 1200$ keV. The final error in τ_m contains a 20% systematic contribution (see text) in addition to the statistical error. Upper (lower) τ_m limits correspond to the average F-value minus (plus) twice the error.

previous determinations exist are given in table 13. The χ^2 value for the F -factors determined at more than one resonance amounts to $\chi^2/(N-n)=0.9(3)$, which shows that the measured F -factors are at least internally consistent.

The results obtained, together with the J^π ; T values for the determination of which they are instrumental, will be discussed in a succeeding paper.

6. Conclusions

The present paper, together with ref. ¹⁾, has shown that the (p, γ) reaction with a Ge detector in a Compton suppression shield can be quite productive for the observation of previously unknown levels, for the determination of branchings and energies of resonances and secondary states, and for the measurement of secondary-state lifetimes.

For the determination of spins and parities the measurement of the angular distribution of the γ -rays produced in (p, γ) reactions can be quite useful, in particular if the spin of the target nucleus is low (e.g. $J_t=0$). For the $^{25}\text{Mg}(p, \gamma)^{26}\text{Al}$ reaction, however, with $J_t=\frac{5}{2}$, the number of parameters entering into the formation of the resonance (channel-spin mixing, orbital momentum mixing) and into its decay (multipole mixing) is generally so large that many γ -ray angular distributions deviate little from isotropy, and that unambiguous J^π determinations become an exception rather than the rule; see e.g. ref. ²⁾.

In a succeeding paper it will be shown that considerations of γ -ray strengths derived from the present resonance strengths, branchings and lifetimes are much more successful for determinations of spins, parities, and also isospins. In this paper also a comparison will be given with a large-scale shell model calculation (for the even-parity states). The astrophysical implications of the present work have been discussed in a separate paper ²⁴⁾.

We are particularly indebted to Dr. H.P. Trautvetter for his willingness to calculate the direct-capture cross-sections, and to many colleagues, students and ex-students for their help and advice in different stages of the present work.

This investigation was performed as part of the research programme of the "Stichting voor Fundamenteel Onderzoek der Materie" (FOM), with financial support from the "Nederlandse Organisatie voor Zuiver-Wetenschappelijk Onderzoek (ZWO)".

References

- 1) P.M. Endt, P. de Wit and C. Alderliesten, Nucl. Phys. **A459** (1986) 61
- 2) E.O. de Neys, M.A. Meyer, J.P.L. Reinecke and D. Reitmann, Nucl. Phys. **A230** (1974) 490
- 3) P.M. Endt, C. Alderliesten and P. de Wit, Phys. Lett. **B173** (1986) 225
- 4) H.J.M. Aarts, C.J. van der Poel, D.E.C. Scherpenzeel, H.F.R. Arciszewski and G.A.P. Engelbertink, Nucl. Instr. Meth. **177** (1980) 417

- 5) R.J. Gehrke, R.G. Helmer and R.C. Greenwood, Nucl. Instr. Meth. **147** (1977) 405
- 6) F. Zijderhand, thesis, Utrecht (1986)
- 7) C. Rolfs, Nucl. Phys. **A217** (1973) 29
- 8) R.R. Betts, H.T. Fortune and D.J. Pullen, Nucl. Phys. **A299** (1978) 412
- 9) H.E. Gove, in Nuclear reactions, ed. P.M. Endt and M. Demeur (North-Holland, Amsterdam, 1959) p. 259
- 10) K. Elix, H.W. Becker, L. Buchmann, J. Görres, K.U. Kettner, M. Wiescher and C. Rolfs, Z. Phys. **A293** (1979) 261
- 11) P.M. Endt and C. van der Leun, Nucl. Phys. **A310** (1978) 1
- 12) P. de Wit, E.L. Bakkum, C. van der Leun and P.M. Endt, Phys. Lett. **113B** (1982) 137
- 13) J. Keinonen, A. Anttila and A. Luukkainen, Nucl. Phys. **A385** (1982) 461
- 14) G.A. Bissinger and C.R. Gould, Particles and Nuclei **3** (1972) 105
- 15) D.L. Show, B.H. Wildenthal, J.A. Nolen and E. Kashy, Nucl. Phys. **A263** (1976) 293
- 16) D.O. Boerma, A.R. Arends, P.M. Endt, W. Grübler, V. König, P.A. Schmelzbach and R. Risler, Nucl. Phys. **A449** (1986) 187
- 17) P.F.A. Alkemade, C. Alderliesten, P. de Wit and C. van der Leun, Nucl. Instr. Meth. **197** (1982) 383
- 18) V. Wijekumar, P. Schmalbrock, H.J. Hausman, T.R. Donoghue, M. Wiescher, H.R. Suiter, C.P. Browne, A.A. Rollefson and R.W. Tarara, Nucl. Phys. **A436** (1985) 561
- 19) C. Alderliesten, J.A. van Nie and A.P. Slok, Nucl. Instr. Meth. to be published
- 20) A.E. Blaugrund, Nucl. Phys. **88** (1966) 501
- 21) S. Kalbitzer, H. Oetzmann, H. Grahmann and A. Feuerstein, Z. Phys. **A278** (1976) 223
- 22) E.L. Bakkum and R.J. Elsenaar, Nucl. Instr. Meth. **227** (1984) 515
- 23) J. Keinonen, B. Nyakó, A. Luukkainen and A. Anttila, Nucl. Phys. **A403** (1983) 45
- 24) P.M. Endt and C. Rolfs, Nucl. Phys. **A467** (1987) 261
- 25) N.J. Davis, J.A. Kuehner, A.J. Trudel and C. Bamber, Phys. Rev. **C33** (1986) 1799
- 26) G. Adams, E.G. Bilpuch, G.E. Mitchell, R.O. Nelson and C.R. Westerfeldt, J. of Phys. **G10** (1984) 1747
- 27) R.J. Peterson, B.L. Clausen, J.J. Kraushaar, H. Nann, W.W. Jacobs, R.A. Lindgren and M.S. Plum, Phys. Rev. **C23** (1986) 31